01 Aug 2024

Meteorological Data Mining and Synthesis for Supplementing On-Site Data for Regulatory Compliance

Ben Sonpon

Shoaib Usman
Missouri University of Science and Technology, usmans@mst.edu

Joseph Smith
Missouri University of Science and Technology, smithjose@mst.edu

Sarah Kovaleski

et. al. For a complete list of authors, see https://scholarsmine.mst.edu/nuclear_facwork/598

Recommended Citation

B. Sonpon et al., "Meteorological Data Mining and Synthesis for Supplementing On-Site Data for Regulatory Compliance," *Energies*, vol. 17, no. 15, article no. 3691, MDPI, Aug 2024.
The definitive version is available at https://doi.org/10.3390/en17153691

energies

MDPI

Article

Meteorological Data Mining and Synthesis for Supplementing On-Site Data for Regulatory Compliance

Ben Sonpon [1], Shoaib Usman [1,*], Joseph Smith [1], Sarah Kovaleski [2] and Jason Wibbenmeyer [2]

[1] Nuclear Engineering and Radiation Science Department, Missouri University of Science and Technology, Rolla, MO 65409, USA; bsg4n@umsystem.edu (B.S.); smithjose@mst.edu (J.S.)
[2] Ameren Callaway Energy Center, 8315 County Rd. 459, Steedman, MO 65077, USA; skovaleski@ameren.com (S.K.); jwibbenmeyer@ameren.com (J.W.)
* Correspondence: usmans@mst.edu

Abstract: Many regulatory requirements add significant delay in the licensing of new nuclear power stations. One area of particular interest is the environmental impact of potential atmospheric release. The purpose of this research is to demonstrate effectiveness of meteorological data mining and synthesis from offsite locations to reduce need for onsite data, hence allowing rapid licensing. The automated procedures tested for data mining and extraction of meteorological data from multiple offsite sources and the data analytic tool developed for data fusion are presented here. Three important meteorological parameters from regulatory compliance are considered for this analysis: wind velocity, wind direction, and atmospheric stability. Callaway Nuclear Power Plant (CNPP) is used as our reference site. CNPP uses the $\frac{\Delta T}{\Delta z}$ approach while we use the Vogt method to estimated stability for the offsite locations. Stability classification correlation coefficients between the reference plant and Columbia Regional Airport range from -0.087 to 0.826 for raw with an average of 0.317 ± 0.313. With travel time, correction changed slightly, i.e., a 10 m observation 0.064 ± 0.249 and 0.028 ± 0.123 and a 60 m observation 0.103 ± 0.265 and 0.063 ± 0.155 for the wind from the reference plant to the airport and vice versa, respectively. For Jefferson City Memorial Airport, raw data correlation was from -0.083 to 0.771, with an average of 0.358 ± 0.321. With travel time, correction changed slightly, i.e., 10 m observation 0.075 ± 0.208 and -0.073 ± 0.255 and 60 m observation 0.018 ± 0.223 and -0.032 ± 0.248 for wind from the reference plant to the airport and vice versa, respectively. Stability classification correlation coefficients between the reference plant and St. Louis Lambert International Airport ranged from -0.083 to 0.763 for raw with an average of 0.314 ± 0.295. With travel time, correction changed slightly, i.e., 10 m observation -0.003 ± 0.307 and -0.030 ± 0.277 and 60 m observation -0.030 ± 0.193 and -0.005 ± 0.215 for wind from the reference plant to the airport and vice versa, respectively. It is important to observe that mathematically. stability class correlation coefficients were not great, but in most cases the predicted and observed values were only off by one stability class. Similar correlations were calculated for wind direction and velocities. Our result, when applied to a proposed nuclear power station, can significantly reduce time and effort to prepare a robust environmental protection plan required for license application.

Keywords: Nuclear Regulatory Commission Compliance; meteorological data; atmospheric stability; data mining; air quality; atmospheric dispersion; Nuclear Reactor Site Licensing

Citation: Sonpon, B.; Usman, S.; Smith, J.; Kovaleski, S.; Wibbenmeyer, J. Meteorological Data Mining and Synthesis for Supplementing On-Site Data for Regulatory Compliance. *Energies* **2024**, *17*, 3691. https://doi.org/10.3390/en17153691

Academic Editor: Dan Gabriel Cacuci

Received: 17 June 2024
Revised: 16 July 2024
Accepted: 23 July 2024
Published: 26 July 2024

1. Introduction

Nuclear power is becoming an integral part of the global energy mix to counter climate change and global warming issues [1]. As the world strives for a decarbonize economy with clean energy, nuclear seems to be the most likely choice for providing reliable, cost-effective, and environmentally friendly electricity [2]. Even some of the oil-rich countries like United Arab Emirates are deploying nuclear as their base-load electric source [3]. However, environmental and safety concerns have been a major roadblock for rapid deployment

of nuclear as a large-scale energy source. Nuclear power is a unique source of energy with multiple competing demands. For nuclear power industry, regulatory demand for environmental safety analysis is far more stringent than any other energy source. In 1950s and 1960s, public support for nuclear energy was strong and the concerns for environmental impacts and human health and safety was not a major consideration. This changed with Three Mile Island [4] and Chernobyl [5] accidents. Public opinion quickly shifted against widespread nuclear power production, and a more stringent regulatory framework evolved, which made nuclear power reactors much safer and at the same time difficult to quickly deploy. For example, in the United States, the US Nuclear Regulatory Commission (NRC) has developed a thorough process of combined license (COL, site license and the operation license) which includes significant public participation. The National Environmental Policy Act (NEPA) [6] and associated regulations such as Environmental Protection Regulations for Domestic Licensing and Related Regulatory Functions (10 CFR Part 51) [7] are to be closely followed for compliance. It is interesting to point out that relative importance of these competing demands is a function of both time and space. For other nations, IAEA Safety Standards [8–11] are available to ensure public health and safety. For a COL application, NRC requires at least 24 consecutive months of meteorological data Regulatory Guide 1.23—Nuclear Regulatory Commission (NRC) [12], while 3 years of data is their preference. This requirement inherently adds 2–3 years of waiting time for any new site application where the site-specific meteorological data are not readily available. However, the same regulation allows for data supplementation since it states "*meteorological conditions pertinent to the site*". Through proper data mining and synthesis, this time can be significantly reduced. By using available data from the surrounding weather stations and developing trustworthy correlation between the available data, the licensee can perform necessary analyses required for environmental impact statement. Our fundamental hypothesis is that offsite data can be synthesized to perform radiological impact analysis for atmospheric pathway.

Likewise, for an operating nuclear power plant, loss of a meteorological tower and data collection ability can have significant economic impacts. NRC requires that at least 90% of the hourly data must be collected and reported to NRC every year [12]. Any instrument failure can lead to power production and hence economic losses. With aging, these failures are becoming frequent, and due to technology obsolescence, repairs are becoming expensive and are often delayed [13]. In extreme cases, the plant might be required to shut down temporarily until reliable meteorological data are restored, resulting in significant financial losses due to halted electric production. Ensuring continuous, reliable meteorological data is thus critical not only for the safe operation of nuclear power plants but also for their economic viability. Therefore, a robust methodology for supplementing meteorological data through data mining and synthesis can significantly improve reliability and cost of electricity from nuclear stations.

The policy of replacing or at least supplementing the on-site meteorological with trustworthy off-site data can significantly accelerate deployment of new reactors as well as can ensure operation of current fleet of nuclear power reactor. For example, in the Environmental Impact Statement attached to Turkey Point's (Units 6 and 7) Combined License Application (COL), meteorological data for the years 2002, 2005, and 2006 were used (application can be seen on the NRC web page). This means that for any new site, at least 3–5 years of meteorological data collection must precede COL application. The system of meteorological data mining and synthesis we are proposing, once fully matured, can significantly reduce this lead time and have a lasting impact on nuclear power industry.

Meteorological data mining and synthesis involve extracting valuable insights and patterns from large volumes of data from a number of relevant sources. This process involves the application of data mining techniques and algorithms to discover hidden patterns, correlations, trends, and relationships within the data [14]. Various fields including energy, environmental monitoring, and risk management use meteorological data mining and synthesis for diverse applications [15]. the ability to predict meteorological data for a given

site using already available data from nearby weather stations can also be very helpful in siting wind farms for renewable energy projects [16]. The optimum wind turbine location can also be determined rapidly by utilizing the results presented here.

For the nuclear power plant licensing process as well as operations, a critical component involves preparing an environmental safety analysis report. According to Regulatory Guide 1.23—Nuclear Regulatory Commission (NRC) [12], at least one meteorological tower must remain operational to collect hourly data, which contributes to the yearly report submitted to the NRC. These data play a vital role in analyzing the radiological impact of potential releases to the environment, potential ground deposition, and possible human intake.

All operational nuclear power plants are mandated to collect hourly Joint Frequency Distribution (JFD) data pertaining to atmospheric stability class, wind direction, and wind speed [17]. These data sets are an important element of the Annual Radioactive Effluent Release report, submitted to NRC to demonstrate compliance with federal regulations. For this study, the Callaway Nuclear power plant in Fulton County Missouri is used as the reference site. Data from the site are acquired to analyze together with publicly available data from nearby weather stations. The Joint Frequency Distribution data in Callaway's 2020 Annual Radioactive Effluent Release Report reveal that, out of 8784 h of valid data, data were successfully collected for 8725 h [17]. Similarly, in their 2021 Annual Radioactive Effluent Release Report, for 8760 h of valid data, Callaway managed to obtain data for 8729 h [18]. Both reports from 2020 and 2021 reveal that Callaway fell short of collecting the complete set of hourly data. This is not an uncommon occurrence; NRC allows a maximum of 10% of missing data annually [12], stating that "*Meteorological instruments should undergo inspections and maintenance at intervals that guarantee a minimum data recovery rate of 90 percent annually*". NRC also allows for supplementing on site, stating "that meteorological conditions at the site and in the surrounding area should be considered in determining the acceptability of a site for a power reactor" [19]. Therefore, any tools or methods to supplement incomplete data through the utilization of data mining techniques and synthesis of meteorological data from neighboring monitoring sites is welcomed by the industry and regulators alike. It is worth noting that despite the unaccounted hours of data in 2020 and 2021, Callaway still met the guidelines outlined in NRC Regulatory Guide 1.23.

The Callaway facility maintains two on-site Met. T designed for the collecting hourly wind speed, wind direction, and air temperatures at two elevations. Using the temperature gradient between the two observation points, atmospheric stability is estimated. In addition, the towers are also collecting dew point/relative humidity data at two specific heights: 10 m and 60 m above ground level. These towers serve a critical role in supporting the facility's efforts to demonstrate compliance with regulatory requirements. To enhance data reliability, Callaway employs two parallel systems, denoted as "A" Alpha and "B" Bravo, ensuring redundancy and establishing a clear hierarchy for data selection, reporting, and analysis [20]. The primary source of on-site meteorological data is the Callaway Met. T. However, it is desirable to supplement and augment these data with information from external sources. Various regional and national resources offer substantial volumes of atmospheric data. With proper synthesis, these off-site data can supplement on-site data for analysis. Our investigation identified multiple dependable data sources close to the Callaway site, all continuously collecting atmospheric data. Unfortunately, these diverse data sets exhibit inconsistencies in terms of data formats, collection frequencies, and naming conventions.

Given the disparities observed in the formatting and nomenclature of atmospheric data obtained from various sources, the first phase of this project focused on developing protocols for automatically importing external data and organizing the data in a consistent format. The next step was comparison of the raw data from various off-site source with on-site data. This comparative analysis was aimed to identify patterns, discrepancies, and trends within the datasets. Lastly, correlations were developed for wind speed (m/s), wind direction (degree), and atmospheric stability between reference plant and off-site sources.

These correlations were developed on a one-to-one basis for each off-site data source and the primary data from the reference plant. To ensure the reliability of the correlation model, historical data were used to validate the correlation model, as well as the data collected during project execution for correlation model validation.

2. Site Geography

The topography and meteorology of a region profoundly influence dispersion patterns [21]. Terrain features such as mountains and coastlines alter airflow, creating wind patterns and turbulence that impact the dispersion of pollutants [22]. Temperature gradients across elevations lead to thermal inversions, trapping pollutants near the surface [23]. Local wind regimes and atmospheric circulation patterns determine the direction and speed of pollutant dispersion [24]. Precipitation and humidity levels also affect pollutant removal from the atmosphere [25], while the boundary layer dynamics govern vertical and horizontal dispersion [26]. Understanding these interactions is crucial for predicting and mitigating air pollution effects on local air quality and public health.

The landscape and geography between the reference plant and the nearby airports, including Columbia Regional Airport, Jefferson City Memorial Airport, and St. Louis Lambert International Airport, exhibit a typical Midwest terrain. The map in Figure 1 shows relative locations of the off-sites and the reference plant. Here, we present a summary of the landscape between these points:

- Columbia Regional Airport (West Northwest of the reference plant):
  - The distance between the reference plant and Columbia Regional Airport is approximately 24 miles and can be characterized by rolling hills and extensive fields. Some of these fields are farmed and others are natural forest typical of Midwest.
  - Columbia itself is situated within a mix of urban and suburban landscapes, featuring residential areas, commercial districts, and the University of Missouri campus.
- Jefferson City Memorial Airport (Southwest of the reference plant):
  - The reference plant lies approximately 23.5 miles away from Jefferson City Memorial Airport. The terrain between these locations may include both rural and semi-urban areas.
  - As the capital city of Missouri, Jefferson City has a scenic location along the Missouri River, offering riverfront views and possibly hilly terrain. Presence of a large river can possibly impact some aspects of meteorological observations and correlations between the reference site and the Jefferson City Memorial Airport.
- St. Louis Lambert International Airport (East of the reference plant):
  - The distance separating the reference plant from St. Louis Lambert International Airport measures approximately 76.37 miles, encompassing a diverse landscape. Traveling from central Missouri to St. Louis, the terrain transitions from rural areas to suburban land and eventually to the urban environment of St. Louis.

The data received from CNPP did not cover all sixteen sectors of the wind rose; instead, they included only eight sectors of the wind rose; north (N), northeast (NE), east (E), southeast (SE), south (S), southwest (SW), west (W), and northwest (NW). Wind speed adjustment was performed by multiplying the measured wind speed by the cosine of the angle of interest relative to the sector midpoint. For instance, if the airport reported wind speed for WNW (292.5 degree), the adjusted wind speed u' for NW sector (315 degree) was calculated using Equation (1):

$$u' = u * cos(\theta) \quad (1)$$

where u is the measured wind speed and θ is the angle between the wind direction and the sector midpoint. In this case, θ = 22.5 degrees (since WNW is 22.5 degrees off from NW).

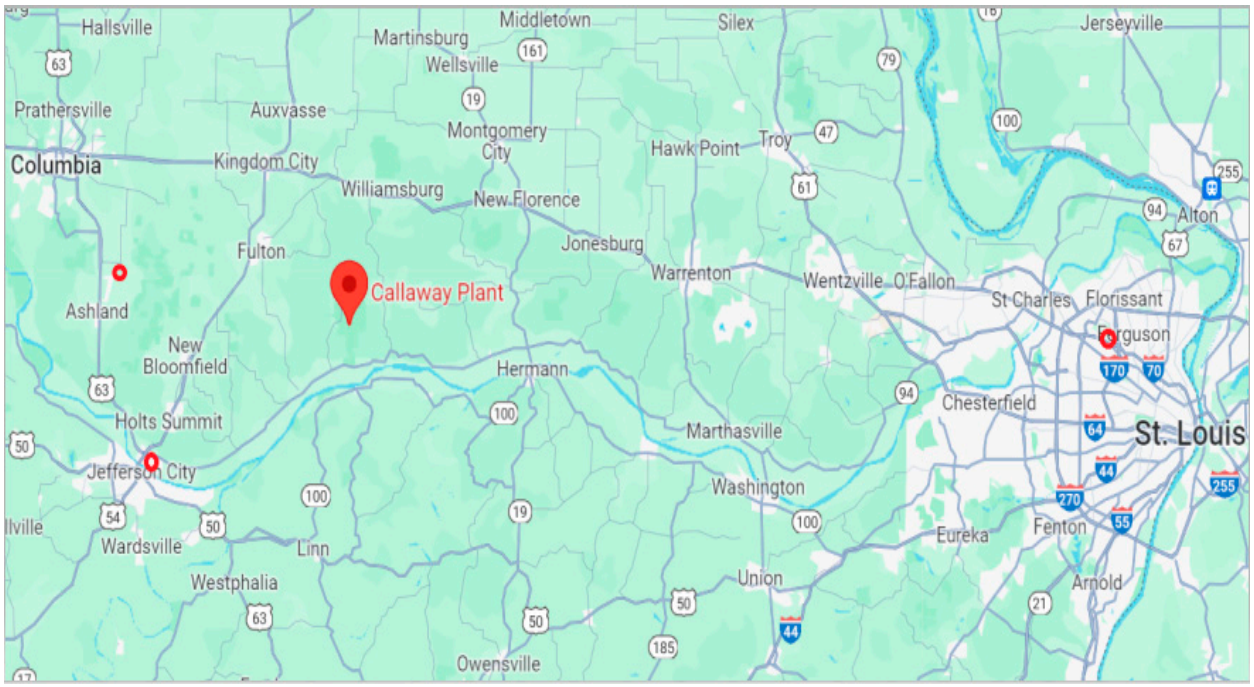

Figure 1. Missouri Map and locations of the reference plant and off-site locations.

Notably, Columbia Regional Airport is situated in the west–northwest of Callaway Nuclear Power Plant. Because of the direction sector resolution difference between airports and our reference power plant, an adjustment was necessary for wind direction and wind speed, particularly for winds traveling in the NW and W directions at a 22.5-degree angle of west–northwest (WNW). Likewise, Callaway Nuclear Power Plant is situated to the east–southeast (ESE) of Columbia Regional Airport. When accounting for winds traveling from Columbia Regional Airport to the Callaway Nuclear Power Plant, we introduced adjustments for wind direction and wind speed, specifically for winds moving in the E and SE directions, and at a 22.5-degree angle from ESE.

Jefferson City Memorial Airport is situated southwest relative to the Callaway Nuclear Power Plant. Therefore, we incorporated adjustments for wind direction and wind speed, especially for winds traveling in the south and west directions at a 45-degree angle from the southwest. For winds moving in the southwest direction, no adjustment for wind direction was necessary as the wind was directly aligned with Jefferson City Memorial Airport. Likewise, Callaway Nuclear Power Plant is located to the northeast of Jefferson City Memorial Airport. When considering winds traveling from Jefferson City Memorial Airport to the Callaway Nuclear Power Plant, we made adjustments for wind direction and wind speed, specifically for winds coming from the east and north directions, and at a 45-degree angle from northeast. For winds moving in the northeast direction, no adjustment for wind direction was needed as the wind was directly aligned with Callaway.

St. Louis Lambert International Airport lies in proximity dead east from Callaway Nuclear Power Plant. Therefore, we account for adjustments in wind direction and wind speed, especially for winds traveling in the northeast and southeast directions at a 45-degree angle from the east. For winds coming from the east direction, no adjustment for wind direction was necessary as the wind was directly aligned with St. Louis Lambert International Airport. Likewise, Callaway Nuclear Power Plant is situated to the west of St. Louis Lambert International Airport. When analyzing winds traveling from St. Louis Lambert International Airport to the Callaway Nuclear Power Plant, we accounted for adjustments in wind direction and wind speed, particularly for winds originating from the northwest and southwest directions, at a 45-degree angle from the west. However, for

winds coming from the west direction, no adjustment for wind direction was necessary as the wind was already aligned with Callaway.

We examined historical data collected at fifteen-minute intervals from Callaway's on-site measurements for wind speed, wind direction, and atmospheric stability, specifically for January 2020, at instrument locations A and B, positioned at heights of 10 m and 60 m above ground level. Of particular importance is atmospheric stability, as it plays a pivotal role in determining turbulence intensity and the diffusion processes that influence the dispersion of effluents into the atmosphere [27]. This relationship is shown in Equation (2), the well-known Gaussian Plume Model, where σ_y and σ_z denote the dispersion coefficients. These coefficients depend on the atmospheric stability class and have a profound impact on the behavior of pollutants in the atmosphere.

$$\Psi = \frac{Q}{2\pi\bar{u}\sigma_y\sigma_z} e^{\left[-\frac{y^2}{2\sigma_y^2}\right]} \left\{ e^{\left[-\frac{(z-H)^2}{2\sigma_z^2}\right]} + e^{\left[-\frac{(z+H)^2}{2\sigma_z^2}\right]} \right\} \quad (2)$$

Q = release rate;
U = wind speed;
H = effective stack height;
$\sigma_{Stability}$ = dispersion coefficient (a function of atmospheric stability).

Atmospheric Stability Classification

Till and Meyer [28] described numerous techniques for inferring atmospheric stability based on meteorological observations. This process involves classifying stability into six or seven distinct categories (lettered A through F, and sometimes G), depending on the method. Each stability class is characterized by its diffusion properties in vertical and transverse directions as a function of travel distance (or time). In most cases, dispersion coefficients are expressed as a function of plume travel distance. At times, rather than using "A", "B", etc., the atmospheric stability is identified by a corresponding integer, ranging from one to six, and sometimes seven. A brief description of various methods used for determining atmospheric stability classes are discussed below.

The first and most commonly used method to determine atmospheric stability is based on the vertical temperature gradient (ΔT). According to the NRC Regulatory Guide 1.23 [12], temperature gradient measurements between 10 m and 60 m provide the required data to estimate the Pasquill Stability Classes. Table 1 provides the temperature gradient ranges and their respective Stability Classes. Callaway, our reference plant, uses this method for determining the stability classes, which is the most common method in the nuclear power industry.

Table 1. Classification of atmospheric stability by vertical temperature difference (NRC) [27].

Stability Classification	Pasquill Categories	Temperature Change with Height (°C/100) m)
Extremely unstable	A	$\Delta T/\Delta z \leq -1.9$
Moderately unstable	B	$-1.9 < \Delta T/\Delta z \leq -1.7$
Slightly unstable	C	$-1.7 < \Delta T/\Delta z \leq -1.5$
Neutral	D	$-1.5 < \Delta T/\Delta z \leq -0.5$
Slightly stable	E	$-0.5 < \Delta T/\Delta z \leq 1.5$
Moderately Stable	F	$1.5 < \Delta T/\Delta z \leq 4.0$
Extremely stable	G	$4.0 < \Delta T/\Delta z$

Adiabatic lapse rate for dry air in the atmosphere is approximately −0.98 °C per 100 m [27]. This means that if the atmosphere demonstrates a lapse rate of −0.98 °C/100 m, a mechanically displaced parcel of air will experience no buoyance force; hence, it is defined as

neutral (Pasquill Class "D"). Any deviation from this lapse rate will either result in unstable or stable atmosphere. When the lapse rate is larger than the adiabatic lapse rate, it enhances mechanically induced turbulence and hence unstable atmosphere. On the other hand, a large negative lapse rate creates an environment where mechanical turbulence is suppressed, leading to a stable atmosphere. Details of this stability classification are shown in Table 1.

The data obtained from our reference site include the following parameters:

- Delta T (ΔT), which represents the temperature difference between 60 m and 10 m, calculated as a one-hour average from Met. T Alpha.
- Delta T (ΔT), similarly measured as the temperature difference between 60 m and 10 m from Met. T Bravo.
- Wind direction and wind speed data at both 60 m and 10 m for Met. T Alpha and Bravo.

As a result of differences in sampling times among the Callaway's plant computer and various servers in use, multiple readings exist for each of the hourly average measurements. Callaway has developed an internal logic to select reconcile these minor differences and provide one average ΔT value for that hour. For example, in Figure 2, there are three values given for midnight, 12:00:09, 12:00:24, and 12:00:28, and the internal computer logic selected ΔT for 12:00:28 as the correct average which is 0.354. This was confirmed by reviewing the 60 m–10 m A ΔT data trend for the time period of 11 P.M. to 12 A.M. We relied on their internal averaging logic to collect our data.

	60-10M A DELTA T 1HR AVG	
Date	CALLAWAY.PCS.RDT5261A	Status
01/01/2020 12:00:09 AM	0.252999991	OK
01/01/2020 12:00:24 AM	0.252999991	OK
01/01/2020 12:00:28 AM	0.354000002	OK
01/01/2020 1:00:09 AM	0.354000002	OK
01/01/2020 1:00:24 AM	0.354000002	OK
01/01/2020 1:00:28 AM	0.652999997	OK
01/01/2020 2:00:09 AM	0.652999997	OK
01/01/2020 2:00:24 AM	0.652999997	OK
01/01/2020 2:00:28 AM	1.057999969	OK
01/01/2020 3:00:09 AM	1.057999969	OK
01/01/2020 3:00:24 AM	1.057999969	OK

Figure 2. Callaway Data Analysis.

NRC does allow for alternate methods of determining atmospheric stability with proper justifications. Some of these alternate methods are discussed in the following paragraphs. One such alternate method is Pasquill stability categories [29] which primarily consider two parameters: surface wind speed and the degree of cloud cover or insolation, see Table 2. Day time cloud cover is divided into strong, moderate, and slight. For the night time, there are only two classes: overcast (cloud cover greater than 3/8) and the other, when the cloud cover is less than or equal to 3/8. Based on the joint occurrence of surface wind speed and cloudiness, the atmospheric stability categories are determined [27].

Another alternate method was proposed by McElroy and co-workers. Table 3 shows the classification of stability classes by McElroy et al., which also considers two key parameters: the bulk Richardson number and Standard deviation of horizontal fluctuation of the wind direction (σ_θ), while their balloons ascend during the experiment. Bulk Richardson number is defined as

$$Ri_B = \frac{g}{T} * \frac{\left(\frac{\partial T}{\partial z} + \Gamma\right) Z^2}{u_{Z^2}} \quad (3)$$

g = acceleration due to gravity;
T = temperature;
Γ = adiabatic lapse rate;
z = height above ground;
u_z = wind speed at the geometrical mean of the heights used to determine the temperature gradient.

Table 2. Pasquill Stability Categories [29].

A: Extremely Unstable Conditions B: Moderately Unstable Conditions C: Slightly Unstable Conditions			D: Neutral Conditions E: Slightly Stable Conditions F: Moderately Stable Conditions		
Surface Wind Speed at 10 m (m/s)	Daytime Insolation			Nighttime Conditions	
	Strong	Moderate	Slight	Thin Overcast or >3/8 Cloudiness	≤3/8 Cloudiness
<2	A	A–B	B		
2–3	A–B	B	C	E	F
3–5	B	B–C	C	D	E
5–6	C	C–D	D	D	D
>6	C	D	D	D	D

Table 3. Definition of Stability classes according to McElroy et al. (1968, 1969) [28,30].

σ_θ (deg)	Richardson Number (Dimensionless)		
	<−0.01	**>0.01**	**±0.01**
24 to 30	B_2' (B) [a]		
24 to 30	B_t' (C)		
15 to 30		C (D)	
8 to 13			D (E)

McElroy and Pooler defined stability classes somewhat differently [30]; however, the corresponding Pasquill stability class is also listed in their table shown here as Table 3.

Another method for inferring atmospheric stability by examining the relations between the Pasquill type and the turbulence criteria R_i and L for flows over low roughness is illustrated in Table 4. This method focuses on two parameters: the Richardson Number and the Monin and Obukhov length. The Monin and Obukhov length is defined as

$$Monin - Obukhov\ Length, L = \frac{u_*^3 C_p \rho T}{kgH} \quad (4)$$

u_* = friction velocity;
ρ = density;
C_p = specific heat at constant pressure;
T = shear stress;
k = von Karman's constant;
g = acceleration due to gravity;
H = vertical heat flux.

Table 4. Relations between Pasquill type and turbulence criteria R_i and L for flow over short grass (Gifford 1976) [31].

Pasquill Type	R_i **(At 2 m)**	**L (m)**
A	−1.0 to −0.7	−2 to −3
B	−0.5 to −0.4	−4 to −5
C	−0.17 to −0.13	−12 to −15
D	0	∞
E	0.03 to 0.05	35 to 75
F	0.05 to 0.11	8 to 35

Table 5 is based on classifying stability according to the standard deviation of horizontal wind direction. This method relies on a single parameter which is the standard deviation of horizontal wind direction. It is common to use 15 min to 1 h data sets to determine standard deviation of horizontal fluctuation.

Table 5. Classification of atmospheric stability by standard deviation of horizontal wind direction (σ_∂) [28].

Stability Classification	Pasquill Categories	σ_θ^b (deg)
Extremely unstable	A	$\sigma_\theta \geq 22.5$
Moderately unstable	B	$22.5 > \sigma_\theta \geq 17.5$
Slightly unstable	C	$17.5 > \sigma_\theta \geq 12.5$
Neutral	D	$12.5 > \sigma_\theta \geq 7.5$
Slightly stable	E	$7.5 > \sigma_\theta \geq 3.8$
Moderately stable	F	$3.8 > \sigma_\theta \geq 2.1$
Extremely stable	G	$2.1 > \sigma_\theta$

Finally, a technique for inferring atmospheric stability using an alternative definition of stability classes as proposed by Vogt [32] is presented below. This is based on solar energy balance. The source of lapse rate is solar energy; hence, it is possible to estimate atmospheric stability using solar energy balance. This method relies on synoptic observations of sun height and cloud cover (insolation index) to estimate the solar energy incident on the earth surface. This information coupled with wind velocity (measured in meters per second) is used to estimate the stability class as shown in Table 6.

Table 6. Alternative definition of the stability classes according to Vogt (1970) [28].

Synoptic Observations	Time of Day	Sun Height, α	Degree of Cloudiness				
	Day	**>50° 31° … 50° 16° … 30° 8° … 15° ≤7°**	**≤4/8**	**5/8 … 7/8 ≤4/8**	**8/8 5/8 … 7/8 ≤4/8**	**8/8 5/8 … 7/8 ≤4/8**	**8/8 >4/8 (0) … 8/8 Fog**
	Night				**8/8**	**5/8–7/8 Fog**	**≤4/8**
Insolation Index	4	3	2	1	0	−1	−2
Measurement of Insolation, cal/cm^2·min	>0.60	0.60 … 0.35	0.34 … 0.16	0.15 … 0.09	0.08 … −0.01	−0.02 … −0.04	≤−0.05
Measurement of Stability [temperature gradient (ΔT/Δz), °C/100 m, measured at height of 120 m and 20 m]	≤−1.5	−1.4 … −1.2	−1.1 … −0.9	−0.8 … −0.7	−0.6 … 0.0	0.1 … 2.0	>2.0
Wind Velocity (u), m/s							
<1	A	A	B	C	D$^+$	G	G
1 … 1.9	A	B	B	C	D$^+$	G	G
2 … 2.9	A	B	C	D	D	E	F
3 … 4.9	B	B	C	D	D	D	E
5 … 6.9	C	C	D	D	D	D	E
≥7	D	D	D	D	D	D	D

It is important to notice that, in addition to stability classes "A" through "G", Vogt adds a "D$^+$" classes which can be described as strongly neutral.

In the Callaway Nuclear Power Plant, our reference site uses the $\frac{\Delta T}{\Delta z}$ method to estimate the atmospheric stability as described in Table 1. On the other hand, most weather stations are not collecting data that can be used to directly infer atmospheric stability. Most airport meteorological stations collect data at five-minute intervals for wind speed, wind direction, and the summation amount layer (degree of cloudiness). These data, coupled with the exact time and date of the observation, can be used to estimate stability. Vogt alternative of stability classes [32] was used in this study to estimate stability for the airports for comparison with the reference plant.

January 2020 was used as an example data set for testing the validity of this approach. The data from three different airports, Columbia Regional Airport, Jefferson City Memorial Airport, and St. Louis Lambert International Airport, were used. These airports were selected due to their proximity to the reference site. Upon analysis, we observed that establishing correlations between on-site and off-site data for wind speed and direction was relatively straightforward. Using the Vogt approach [32], one can develop a complete data set (wind velocity, direction, and atmospheric stability) for the airport which can then be used for comparison and correlation development.

To calculate solar energy received by the earth's surface in addition to the longitude and latitude of the location of interest, information about the day of the year and time of day is essential. The measurement of the sun's height in the sky relative to the horizontal is referred to as the sun height angle or the sun elevation angle (Figure 3). At sunrise and sunset, this angle is 0°, while the maximum elevation angle is reached at solar noon [33]. Equation (5) is used to determine the sun elevation angle, which is influenced by the latitude (φ) of the location, the declination angle (δ), dependent on the day of the year and varying every season due to the earth rotation around the sun and the earth on its axis of rotation, and the hour angle, which accounts for a local solar time conversion to the number of degrees the sun travels across the sky [33]. Notably, the declination angel follows distinct patterns: it registers at zero during the equinoxes, observed on 22 March and 22 September. In the northern hemisphere, it assumes positive values during summer and negative values during winter. The declination angle attains its maximum, peaking at 23.45 degrees, on 22 June. Conversely, it reaches its minimum, hitting −23.45 degrees, around 21–22 December [33]. Equations (6) and (7) are used to calculate the declination angle and the hour angle, respectively. In addition, Table 7 provides the definition of sky cover, with each layer presented in the following format: ccc:ll-xxx, where "ccc" represents coverage, "ll" signifies layer, and "xxx" (not displayed in Table 7) denotes the cloud base height at the lowest point of the layer [34].

$$\alpha = sin^{-1}[\sin\delta\sin\varphi + \cos\delta\cos\varphi\cos(HRA)] \tag{5}$$

$$\delta = -23.45^0 \times \cos\left(\frac{360}{365} \times (d+10)\right) \tag{6}$$

$$HRA = 15^0 \times (LST - 12) \tag{7}$$

When establishing correlations, typically, data points are observed at the same time. However, in our dataset, this is not possible. A time discrepancy exists between the data recorded at the reference plant and the data obtained from off-site weather stations. This temporal misalignment could be attributed to factors such as wind travel time, wind speed variations, surface roughness, and more. To address the wind travel time between the reference plant and the various weather stations, we initially take into consideration three key factors: the distance, the wind speed measured at the recorded time, and wind direction.

$$Travel\ Time = \frac{Distance}{Effective\ Wind\ Speed} = \frac{Distance}{Wind\ Speed \times \cos\theta} \tag{8}$$

where the effective wind speed is adjusted for the direction of travel using the cosine of the angle between wind direction and reference direction. The estimated time at which the

wind, originating from the reference plant, reaches the weather station or vice versa is the arrival time. Arrival time is computed by adding travel time to recorded time.

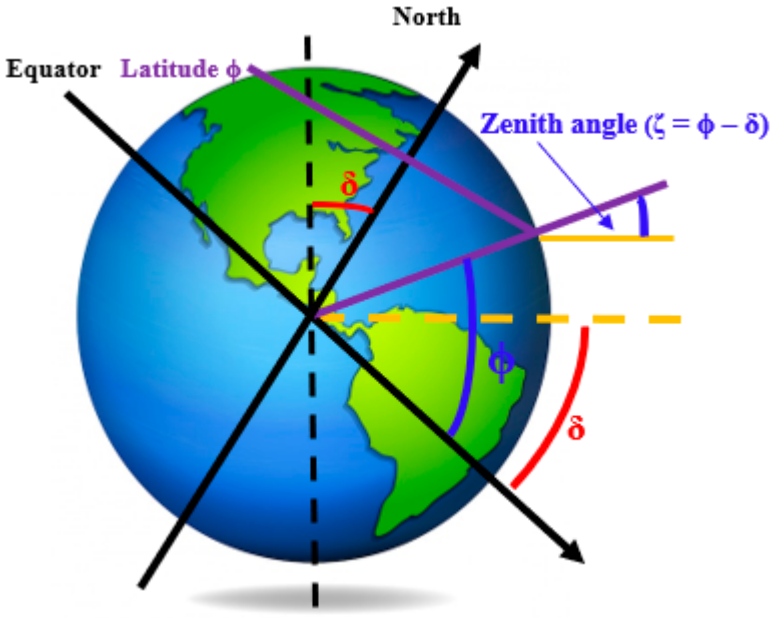

Figure 3. Solar energy balance showing elevation and declination angles.

Table 7. Contraction for Sky Cover (Local Climatological Data) [34].

Reportable Contraction (ccc)	Meaning	Summation Amount of Layer (ll)
VV	Vertical Visibility	8/8
SKC or CLR	Clear	0
FEW	Few	1/8–2/8
SCT	Scattered	3/8–4/8
BKN	Broken	5/8–7/8
OVC	Overcast	8/8

Wind velocities are measured at a 10 m height for open terrain and a 20 m height for areas with tree and forestry cover [35]. To obtain appropriate wind velocity data for stability calculation, a Python code was developed to compute both travel time and arrival time. This model also matches the arrival time data with the nearest available data points in the destination file, typically within a 5–10 min interval, as part of the correlation development process. Importantly, this process takes into consideration the fact that wind speed is not constant during the entire journey. The data collected from the various airports were obtained at a height of 10 m. Consequently, when comparing these data with the Callaway data, which are also measured at 60 m, we need to consider adjustments for both height and wind speed. Equation (9) is utilized to incorporate a height correction factor when comparing the data obtained from the airports at a 10 m height to the Callaway data, which are collected at a height of 60 m. In this equation, "β" is vertical wind profile correction exponent, which varies based on the surface roughness, and hence stability class [35] "z_0" represents the reference height (in our study, it is 10 m above undisturbed terrain), "$u(z_0)$" stands for the wind speed at "z_0," and "z" denotes the height of interest, in our case, 60 m.

$$u(z) = u(z_0) * \left(\frac{z}{z_0}\right)^{\beta} \quad (9)$$

However, once we apply Equation (9) to make the necessary height and wind speed adjustments, it is essential to understand that the wind directions are assumed to remain consistent with those observed at 10 m at the various airports. While we account for height corrections, we anticipate that wind speed will increase with higher elevations. But we assume that there is no change in the stability from a 10 m elevation to a 60 m elevation, since the speed correction was made based on a stability classification at 10 m. Below, Table 8 shows the different "m" values corresponding to the stability classes outlined by Environmental Protection Agency.

Table 8. Exponents of the vertical wind profile [28].

Diffusion Category	Wind Profile Exponents, m_j	
A (j = 6)	0.09	0.10
B (j = 5)	0.20	0.15
C (j = 4)	0.22	0.20
D (j = 3)	0.28	0.25
E (j = 2)	0.37	0.30
F (j = 1)	0.42	0.30

3. Results

Hourly atmospheric stability, wind speed, and wind direction assessments were acquired from Columbia Regional Airport, St. Lambert International Airport, and Jefferson City Memorial Airport for the months of January, May, and September. These airport locations were chosen due to their proximity to the Callaway Nuclear Power Plant, and the three months (January, May, and September) were chosen to account for seasonal variations. Given the volume of data, only January 2020 data are included in the discussion here and only for the reference site (CNPP) and the three offsite locations for demonstration purpose. In a real-world situation, the correlations as presented here would have to be constantly revised as new meteorological data from reference site as well as selected offsite would become available. Furthermore, it is quite possible that one may need to develop these correlations with seasonal dependence. For example, for winter months (particularly when the ground is covered with snow), a correlation for stability category may need revision, etc. It is also important to recognize the fact that our study is limited to only one reference site and three offsite locations and is specific to this combination. For every new site, a similar yet new correlation has to be developed, specific to site condition using the methodology presented here.

It is worth noticing that while factoring in wind direction travel in our correlation calculations, we observed instances where the wind did not follow the trajectory toward the relevant airport of interest on certain days.

Presented below are tables and graphs displaying examples of the computed atmospheric stability data for both Columbia Regional Airport and estimated stability at Callaway Nuclear Power Plant Met. T Alpha using the $\frac{\Delta T}{\Delta z}$ method. The graph for the month of January and the correlation coefficients for each day's data between Callaway and Columbia Regional Airport is included in Appendix B. Each table presents a detailed overview of meteorological conditions at Callaway and various airports. Callaway's wind patterns, including both numerical and lettered wind direction, along with hourly wind speeds at 10 and 60 m, are included. The corresponding atmospheric stability classes, identified by letters (A–G), are linked to travel times and arrival times, providing insights into the temporal dynamics of stability classes. Importantly, the stability classes are numerically characterized, adding a layer of information to the analysis. For airport sites, calculation-based estimated data such as solar elevation corrected for atmospheric refraction, hourly wind direction, and wind speed at 10 and 60 m are included for a better understanding of atmospheric conditions.

Table 9 illustrates that on 1 January, specifically at a height of 10 m, the wind from the Callaway Nuclear Power Plant was observed to be directed towards Columbia Regional Airport only once during that day. Conversely, there was no wind traveling in the direction of Callaway from Columbia Regional Airport at 10 m. Figures 4–6 display graphs of

atmospheric stability, wind speed, and wind direction for wind traveling from CNPP to CRA at 60 m (data shown in Table 10).

Table 9. Atmospheric Data for Callaway Nuclear Power Plant to Columbia Regional Airport for 1 January with Adjustments for Travel Time and Wind Direction at 10 m at Met. T Alpha.

Callaway Time	Callaway Wind Direction in Number 10 m (A)	Callaway Hourly Wind Speed (m/s) at 10 m (A)	Callaway Stability (ΔT) [a] 60 m and 10 m	Travel Time	Arrival Time	Columbia Regional Airport time	CRA Solar Elevation Corrected for atm refraction (deg)	CRA Hourly Wind Direction (deg)	CRA Wind Speed (m/s)	CRA Stability
1 January 2020 00:00:00	265.1 (W) [b]	3.4	E (5)	0 days 03:22:39	1 January 2020 03:22:40	1 January 2020 03:20:31	−58.5	180 (S [b])	2.2	F (6)

[a] Temperature variation with height (same footnote for Tables 10–15). [b] Best estimate for the wind direction (same footnote for Tables 10–15).

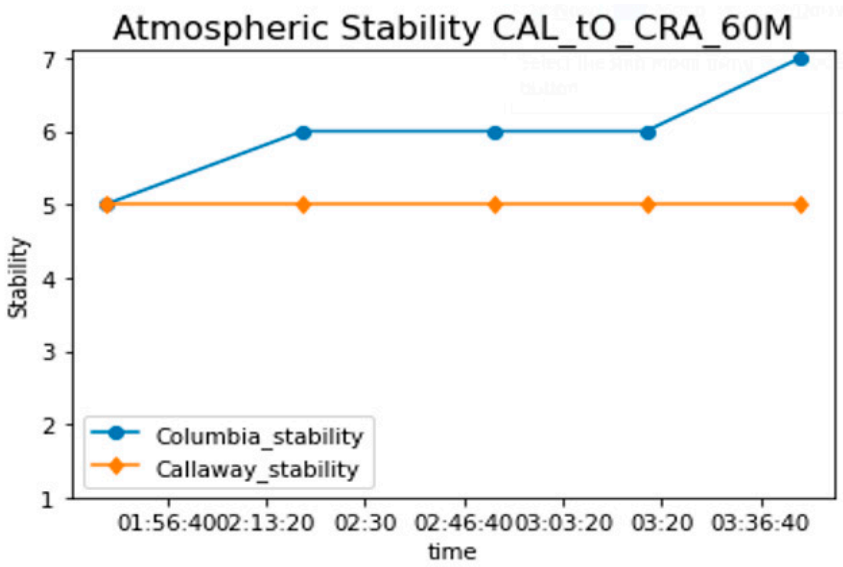

Figure 4. Atmospheric Stability Graph for wind travelling from Callaway to Columbia Regional Airport at 60 m (1 January 2020, data).

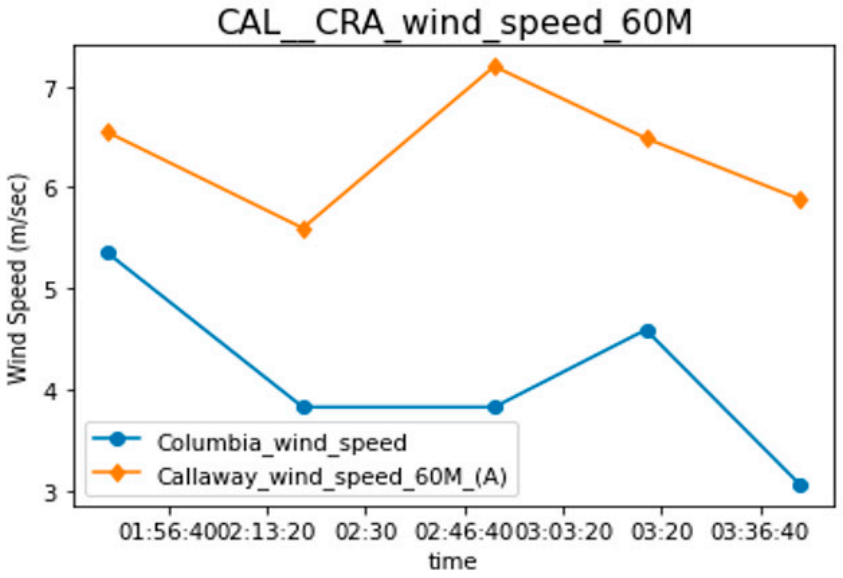

Figure 5. Wind Speed Graph for wind travelling from Callaway to Columbia Regional Airport at 60 m (1 January 2020, data).

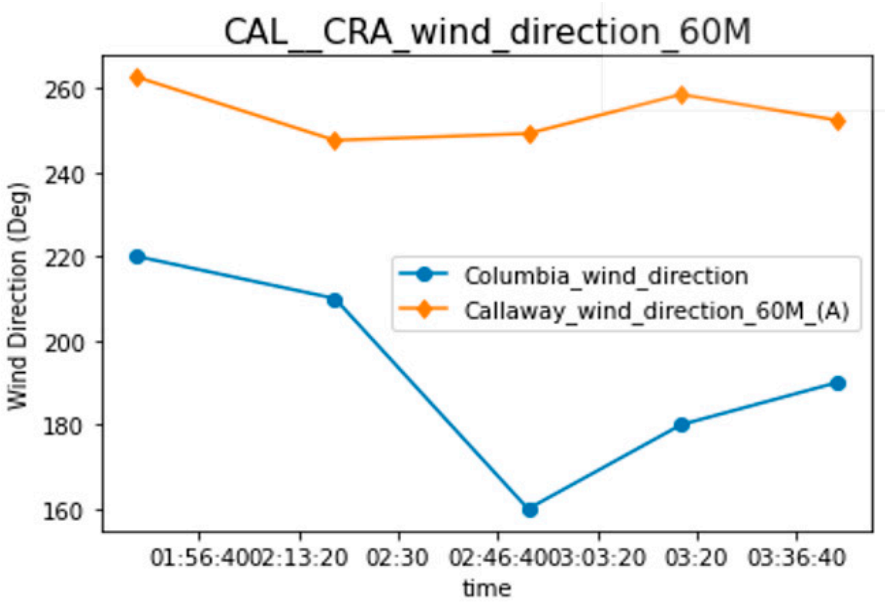

Figure 6. Wind Direction Graph for wind travelling from Callaway to Columbia Regional Airport at 60 m (1 January 2020, data).

Table 10. Atmospheric Data for Callaway Nuclear Power Plant to Columbia Regional Airport for 1 January with Adjustments for Travel Time and Wind Direction at 60 m at Met. T Alpha.

Callaway Time	Callaway Wind Direction in Number 60 m (A)	Callaway Hourly Wind Speed (m/s) at 60 m (A)	Callaway Stability (ΔT) [a] 60 m and 10 m	Travel Time	Arrival Time	Columbia Regional Airport Time	CRA Solar Elevation Corrected for Atm Refraction (deg)	CRA Hourly Wind Direction (deg)	CRA Wind Speed (m/s)	CRA Stability
1 January 2020 00:00:00	262.6 (W [b])	6.5	E (5)	0 days 01:46:21	1 January 2020 01:46:21	1 January 2020 01:45:31	−72.7	220 (SW [b])	5.4	E (5)
1 January 2020 00:15:00	247.6 (W [b])	5.6	E (5)	0 days 02:04:26	1 January 2020 02:19:27	1 January 2020 02:15:31	−69.2	210 (SW [b])	3.8	F (6)
1 January 2020 01:15:00	249.2 (W [b])	7.2	E (5)	0 days 01:36:46	1 January 2020 02:51:46	1 January 2020 02:50:31	−63.8	160 (S [b])	3.8	F (6)
1 January 2020 01:30:00	258.5 (W [b])	6.5	E (5)	0 days 01:47:22	1 January 2020 03:17:23	1 January 2020 03:15:31	−59.4	180 (S [b])	4.6	F (6)
1 January 2020 01:45:00	252.4 (W [b])	5.9	E (5)	0 days 01:58:23	1 January 2020 03:43:24	1 January 2020 03:40:31	−54.8	190 (S [b])	3.1	G (7)

[a] Temperature variation with height. [b] Best estimate for the wind direction.

Within the context of this analysis, this prediction is quite satisfactory because it demonstrates good agreement between our calculated atmospheric stability and the observed stability at Callaway Plant. For most of the observations, our estimates are only off by one stability class. Table 11 contains similar data for Columbia Regional Airport and Callaway Nuclear Power Plant without adjustment for wind direction and travel time correction.

Just as in the case of the computed atmospheric data at 10 m from Columbia Regional Airport to Callaway, there was no wind observed to be moving in the direction from Columbia Regional Airport to Callaway at a height of 60 m for 1 January.

Table 11. Atmospheric Data for Columbia Regional Airport and Callaway Nuclear Power Plant for January 1 without Adjustments for Travel Time and Wind Direction at 60 m at Met T. Alpha.

Columbia Regional Airport Time	CRA Solar Elevation Corrected for Atm Refraction (deg)	CRA Hourly Wind Direction (deg)	CRA Wind Speed (m/s) at 10 m	CRA Wind Speed (m/s) at 60 m	CRA STABILITY Letter	Callaway Date and Time	Callaway 10 m A WIND DIR 1 HR AVG	Callaway Hourly Wind Speed (m/s) at 10 m	Callaway 60 m A WIND DIR 1 HR AVG	Callaway Hourly Wind Speed (m/s) at 60 m	Callaway Stability (ΔT) [a] 60 m & 10 m
00:54:00	−73.8	220 (SW [b])	3.1	5.4	E (5)	1 January 2020 1:00:28 A.M.	229.2 (SW [b])	2.4	229.2 (SW [b])	5.9	E (5)
01:54:00	−71.9	220 (SW [b])	4.0	6.9	E (5)	1 January 2020 2:00:28 A.M.	233.3 (SW [b])	2.6	233.3 (W [b])	6.5	E (5)
02:54:00	−63.2	170 (S [b])	3.1	5.4	E (5)	1 January 2020 3:00:28 A.M.	223.8 (SW [b])	2.5	223.8 (SW [b])	6.5	E (5)
03:54:00	−52.3	180 (S [b])	2.7	4.6	F (6)	1 January 2020 4:00:28 A.M.	219.6 (SW [b])	2.4	219.6 (SW [b])	6.3	E (5)
04:54:00	−40.7	180 (S [b])	3.6	6.1	E (5)	1 January 2020 5:00:28 A.M.	165 (S [b])	0.7	165 (SW [b])	4.7	E (5)
05:54:00	−29.0	160 (S [b])	3.6	6.1	E (5)	1 January 2020 6:00:28 A.M.	179.8 (S [b])	2.7	179.8 (S [b])	6.5	F (6)
06:54:00	−17.6	170 (S [b])	2.7	4.6	F (6)	1 January 2020 7:00:28 A.M.	166.1 (S [b])	3.0	166.1 (S [b])	6.4	F (6)
07:54:00	−6.6	190 (S [b])	4.0	6.9	E (5)	1 January 2020 8:00:28 A.M.	162.4 (S [b])	3.3	162.4 (S [b])	6.9	F (6)
08:54:00	3.8	200 (S [b])	4.9	7.7	D (4)	1 January 2020 9:00:28 A.M.	181.8 (S [b])	3.7	181.8 (S [b])	7.3	E (5)
09:54:00	12.8	210 (SW [b])	6.3	9.8	D (4)	1 January 2020 10:00:28 A.M.	195.7 (S [b])	4.4	195.7 (SW [b])	6.7	D (4)
10:54:00	20.3	200 (S [b])	6.7	10.5	D (4)	1 January 2020 11:00:28 A.M.	211.6 (SW [b])	4.6	211.6 (SW [b])	6.8	D (4)
11:54:00	25.6	210 (SW [b])	7.2	11.2	D (4)	1 January 2020 12:00:28 P.M.	218.1 (SW [b])	5.3	218.1 (SW [b])	7.7	D (4)
12:54:00	28.1	200 (S [b])	9.4	14.7	D (4)	1 January 2020 1:00:28 P.M.	211.9 (SW [b])	5.7	211.9 (SW [b])	8.2	D (4)
13:54:00	27.5	200 (S [b])	10.3	16.1	D (4)	1 January 2020 2:00:28 P.M.	205.7 (SW [b])	6.5	205.7 (SW [b])	9.2	D (4)
14:54:00	23.8	190 (S [b])	8.9	14.0	D (4)	1 January 2020 3:00:28 P.M.	193.9 (S [b])	6.6	193.9 (S [b])	9.0	D (4)

Table 11. *Cont.*

Columbia Regional Airport Time	CRA Solar Elevation Corrected for Atm Refraction (deg)	CRA Hourly Wind Direction (deg)	CRA Wind Speed (m/s) at 10 m	CRA Wind Speed (m/s) at 60 m	CRA STABILITY Letter	Callaway Date and Time	Callaway 10 m A WIND DIR 1 HR AVG	Callaway Hourly Wind Speed (m/s) at 10 m	Callaway 60 m A WIND DIR 1 HR AVG	Callaway Hourly Wind Speed (m/s) at 60 m	Callaway Stability (ΔT) [a] 60 m & 10 m
15:54:00	17.6	190 (S [b])	6.7	10.5	D (4)	1 January 2020 4:00:28 P.M.	190.6 (S [b])	5.9	190.6 (S [b])	8.3	E (5)
16:54:00	9.5	180 (S [b])	6.7	10.5	D (4)	1 January 2020 5:00:28 P.M.	183.5 (S [b])	6.1	183.5 (S [b])	9.0	E (5)
17:54:00	0.3	170 (S [b])	5.8	9.1	D (4)	1 January 2020 6:00:24 P.M.	181.2 (S [b])	5.4	181.2 (S [b])	8.4	E (5)
18:54:00	−10.8	180 (S [b])	4.9	8.4	E (5)	1 January 2020 7:00:24 P.M.	178.8 (S [b])	5.3	178.8 (S [b])	8.2	E (5)
19:54:00	−21.9	190 (S [b])	6.7	11.5	E (5)	1 January 2020 8:00:24 P.M.	185.9 (S [b])	6.2	185.9 (S [b])	9.3	E (5)
20:54:00	−33.5	190 (S [b])	6.3	10.7	E (5)	1 January 2020 9:00:24 P.M.	181.8 (S [b])	5.3	181.8 (S [b])	8.2	E (5)
21:54:00	−45.2	190 (S [b])	4.5	7.7	E (5)	1 January 2020 10:00:24 P.M.	181.8 (S [b])	5.0	181.8 (S [b])	8.0	E (5)
22:54:00	−56.6	180 (S [b])	4.9	8.4	E (5)	1 January 2020 11:00:24 P.M.	179.3 (S [b])	4.6	179.3 (S [b])	7.6	E (5)
23:54:00	−67.0	180 (S [b])	6.3	10.7	E (5)						

[a] Temperature variation with height (same footnote for Tables 10–15). [b] Best estimate for the wind direction (same footnote for Tables 10–15).

Taking into account that atmospheric stability remains constant at both 10 m and 60 m without wind direction, travel time, and correction, Figure 7 displays the atmospheric stability graph comparing the offsite calculated stability values using the Vogt method of inferring atmospheric stability for the airport and the ΔT method for the reference plant. Again, the predictions are off by a maximum of one stability class, which is quite good.

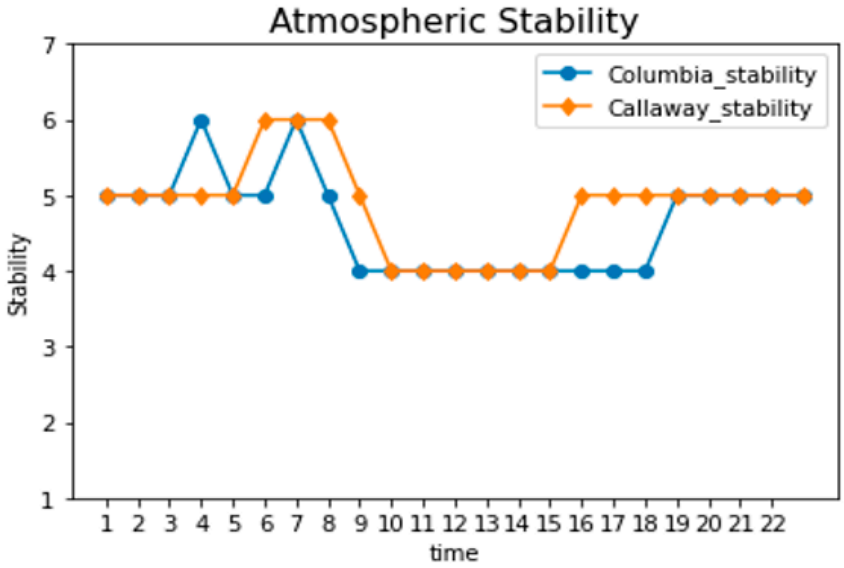

Figure 7. Atmospheric Stability Graph for Callaway and Columbia Regional Airport at 10 and 60 m without Adjustments for Travel Time and Wind Direction (1 January 2020, data).

Figure 8 shows the comparison of wind direction between our reference plant (Callaway) and Columbia airport. It is worth noticing that for the same location, the recorded wind direction at 10 m does not match exactly with the 60 m observation. Given this level of data spread, the correlation between the two sites is quite good.

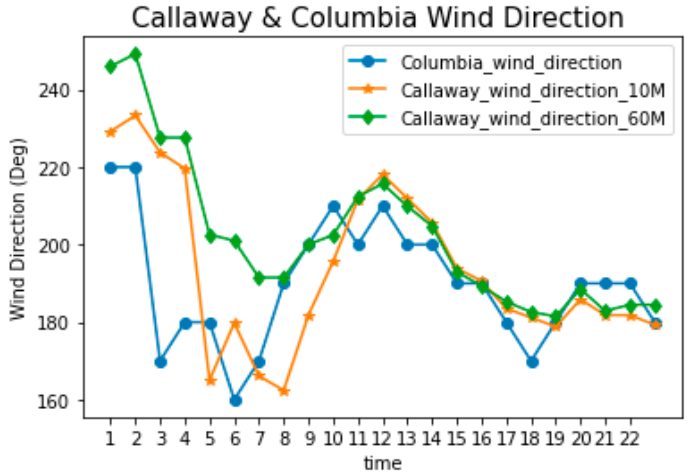

Figure 8. Wind Direction Graph for Callaway and Columbia Regional Airport at 10 and 60 m without Adjustments for Travel Time and Wind Direction.

Table 12 and Figures 9–11 display examples of computed atmospheric stability, wind velocity, and direction data for 19 January when wind was traveling from Callaway to Jefferson City Memorial Airport. Only two records were found for this wind direction for 19 January 2020. Table 13 shows the data for 19 January 2020, when the wind was coming to Callaway from Jefferson City Memorial Airport. A total of 20 observations were made for this condition. Figures 12–14 show comparison of the two sites. With the exception of

wind direction, good correlation was observed. Due to limited space, only January 19 data are presented in detail; the remaining data re included in Appendix C.

Table 12. Atmospheric Data for Callaway Nuclear Power Plant to Jefferson City Memorial Airport for 19 January with Adjustments for Travel Time and Wind Direction at 60 m at Met. T Alpha.

Callaway Time	Callaway Wind Direction in Number 60 m (A)	Callaway Hourly Wind Speed (m/s) at 60 m (A)	Callaway Stability (ΔT) [a] 60 m and 10 m	Travel Time	Arrival Time	Jefferson City Memorial Airport Time	JMA Solar Elevation Corrected for Atm Refraction (deg)	JMA Hourly Wind Direction (deg)	JMA Wind Speed (m/s)	JMA Stability Letters
19 January 2020 12:30:00	292.3 (W [b])	6.1	D (4)	0 days 03:49:55	19 January 2020 16:19:56	19 January 2020 16:15:31	18.1	310 (NW [b])	4.5	C (3)
19 January 2020 13:00:00	285.2 (W [b])	5.7	D (4)	0 days 04:23:28	19 January 2020 17:23:28	19 January 2020 17:20:31	8.5	300 (NW [b])	4.0	D (4)

[a] Temperature variation with height (same footnote for Tables 10–15). [b] Best estimate for the wind direction (same footnote for Tables 10–15).

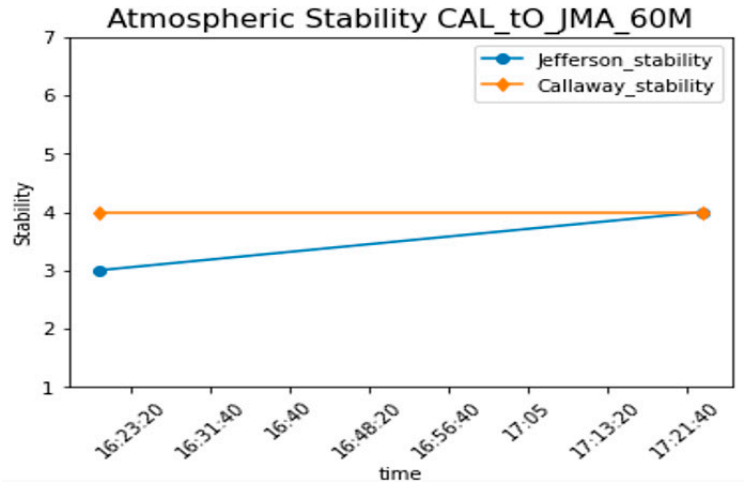

Figure 9. Atmospheric Stability Graph for wind travelling from Callaway to Jefferson City Memorial Airport at 60 m (19 January 2020, data).

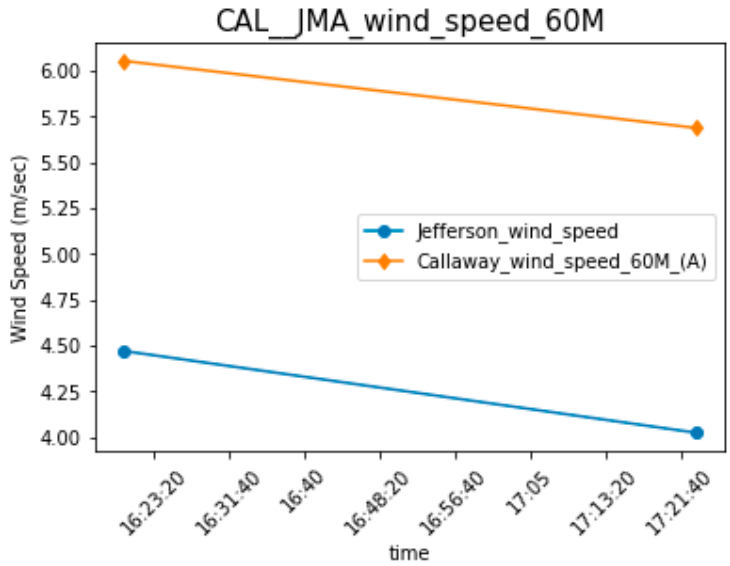

Figure 10. Atmospheric Stability Graph for wind travelling from Callaway to Jefferson City Memorial Airport at 60 m (19 January 2020, data).

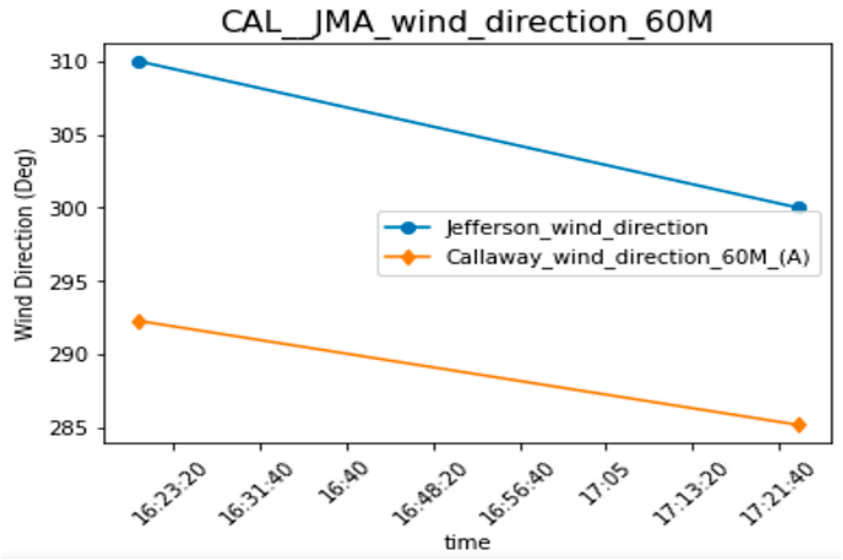

Figure 11. Atmospheric Stability Graph for wind travelling from Callaway to Jefferson City Memorial Airport at 60 m (19 January 2020, data).

Table 13. Atmospheric Data for Jefferson City Memorial Airport to Callaway Nuclear Power Plant for January 19 with Adjustments for Travel Time and Wind Direction at 60 m at Met. T Alpha.

Jefferson City Memorial Airport Time	JMA Solar Elevation Corrected for Atm Refraction (deg)	JMA Hourly Wind Direction (deg)	JMA Wind Speed (m/s)	JMA Stability	Travel Time	Arriva Time	Callaway Time	Callaway Wind Direction in Number 60 m (A)	Callaway Hourly Wind Speed (m/s) at 60 m (A)	Callaway Stability (ΔT) [a] 60 m and 10 m
19 January 2020 19:35:31	−15.5	340 (N [b])	6.9	E (5)	0 days 02:09:32	19 January 2020 21:45:04	19 January 2020 21:45:00	336.5 (NW [b])	4.6	E (5)
19 January 2020 19:30:31	−14.6	340 (N [b])	5.4	E (5)	0 days 02:46:33	19 January 2020 22:17:05	19 January 2020 22:15:00	325.7 (NW [b])	3.6	E (5)
19 January 2020 20:30:31	−26.1	340 (N [b])	7.7	E (5)	0 days 01:56:35	19 January 2020 22:27:07	19 January 2020 22:15:00	325.7 (NW [b])	3.6	E (5)
19 January 2020 20:35:31	−27.1	340 (N [b])	7.7	E (5)	0 days 01:56:35	19 January 2020 22:32:06	19 January 2020 22:30:00	335.1 (NW [b])	3.6	E (5)
19 January 2020 19:55:31	−19.3	340 (N [b])	5.4	E (5)	0 days 02:46:33	19 January 2020 22:42:04	19 January 2020 22:30:00	335.1 (NW [b])	3.6	E (5)
19 January 2020 20:40:31	−28.0	340 (N [b])	6.9	E (5)	0 days 02:09:32	19 January 2020 22:50:04	19 January 2020 22:45:00	331.2 (NW [b])	4.1	E (5)
19 January 2020 20:05:31	−21.3	340 (N [b])	5.4	E (5)	0 days 02:46:33	19 January 2020 22:52:04	19 January 2020 22:45:00	331.2 (NW [b])	4.1	E (5)
19 January 2020 20:10:31	−22.2	340 (N [b])	5.4	E (5)	0 days 02:46:33	19 January 2020 22:57:05	19 January 2020 22:45:00	331.2 (NW [b])	4.1	E (5)
19 January 2020 20:20:31	−24.2	340 (N [b])	5.4	E (5)	0 days 02:46:33	19 January 2020 23:07:05	19 January 2020 23:00:00	331.2 (NW [b])	3.0	E (5)
19 January 2020 19:25:31	−13.6	340 (N [b])	3.8	F (6)	0 days 03:53:11	19 January 2020 23:18:42	19 January 2020 23:15:00	332.3 (NW [b])	3.7	E (5)
19 January 2020 20:45:31	−29.0	340 (N [b])	5.4	E (5)	0 days 02:46:33	19 January 2020 23:32:04	19 January 2020 23:30:00	344.1 (N [b])	3.6	E (5)

Table 13. *Cont.*

Jefferson City Memorial Airport Time	JMA Solar Elevation Corrected for Atm Refraction (deg)	JMA Hourly Wind Direction (deg)	JMA Wind Speed (m/s)	JMA Stability	Travel Time	Arriva Time	Callaway Time	Callaway Wind Direction in Number 60 m (A)	Callaway Hourly Wind Speed (m/s) at 60 m (A)	Callaway Stability (ΔT) [a] 60 m and 10 m
19 January 2020 20:50:31	−30.0	350 (N [b])	5.4	E (5)	0 days 02:46:33	19 January 2020 23:37:04	19 January 2020 23:30:00	344.1 (N [b])	3.6	E (5)
19 January 2020 20:25:31	−25.1	340 (N [b])	4.6	F (6)	0 days 03:14:19	19 January 2020 23:39:50	19 January 2020 23:30:00	344.1 (N [b])	3.6	E (5)
19 January 2020 20:55:31	−31.0	350 (N [b])	5.4	E (5)	0 days 02:46:33	19 January 2020 23:42:05	19 January 2020 23:30:00	344.1 (N [b])	3.6	E (5)
19 January 2020 21:00:31	−32.0	340 (N [b])	5.4	E (5)	0 days 02:46:33	19 January 2020 23:47:05	19 January 2020 23:45:00	337.4 (NW [b])	4.2	E (5)
19 January 2020 21:30:31	−37.8	350 (N [b])	6.1	E (5)	0 days 02:25:44	19 January 2020 23:56:15	19 January 2020 23:45:00	337.4 (NW [b])	4.2	E (5)
19 January 2020 21:35:31	−38.8	340 (N [b])	6.1	E (5)	0 days 02:25:44	20 January 2020 00:01:15	20 January 2020 00:00:00	337.9 (N [b])	4.5	E (5)
19 January 2020 21:25:31	−36.8	340 (N [b])	5.4	E (5)	0 days 02:46:33	20 January 2020 00:12:04	20 January 2020 00:00:00	337.9 (N [b])	4.5	E (5)
19 January 2020 21:40:31	−39.8	340 (N [b])	5.4	E (5)	0 days 02:46:33	20 January 2020 00:27:05	20 January 2020 00:15:00	348.8 (N [b])	4.5	E (5)
19 January 2020 22:10:31	−45.6	340 (N [b])	6.1	E (5)	0 days 02:25:44	20 January 2020 00:36:15	20 January 2020 00:30:00	351.8 (N [b])	3.7	E (5)

[a] Temperature variation with height (same footnote for Tables 10–15). [b] Best estimate for the wind direction (same footnote for Tables 10–15).

Table 14 and Figure 15 display examples of computed atmospheric stability for January 2 when the wind was traveling from Callaway to St. Louis Lambert International Airport. Only six records were found for this wind direction for 2 January 2020. Table 15 shows the data for 2 January 2020, when the wind was coming to Callaway from Lambert Airport. A total of seven observations were made for this condition. Figure 16 shows the comparison of the two sites for stability class. The remaining data are included in Appendix D.

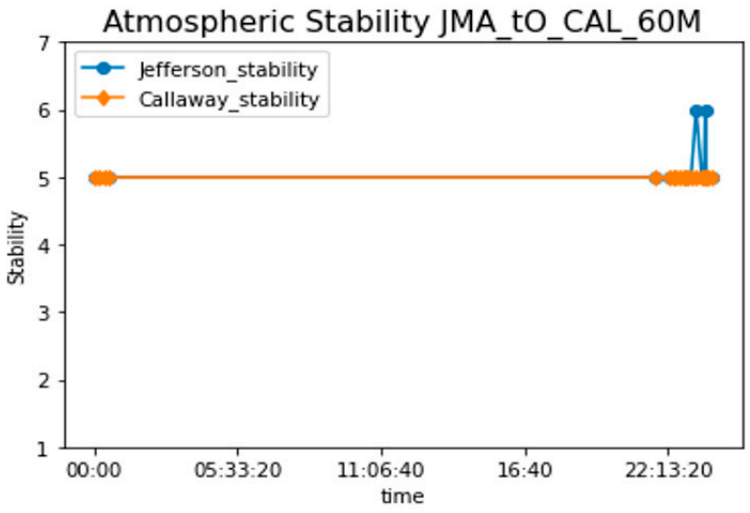

Figure 12. Atmospheric Stability Graph for wind travelling from Jefferson City Memorial Airport to Callaway at 60 m (19 January 2020, data).

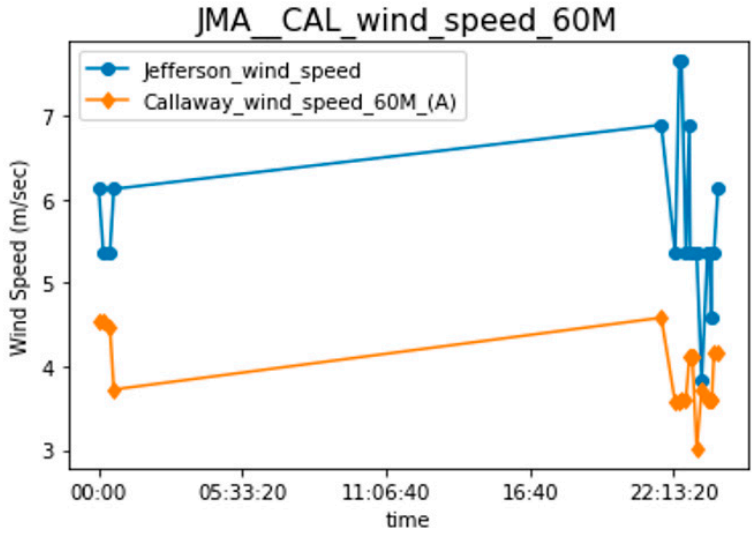

Figure 13. Wind Speed Graph for wind travelling from Jefferson City Memorial Airport to Callaway at 60 m (19 January 2020, data).

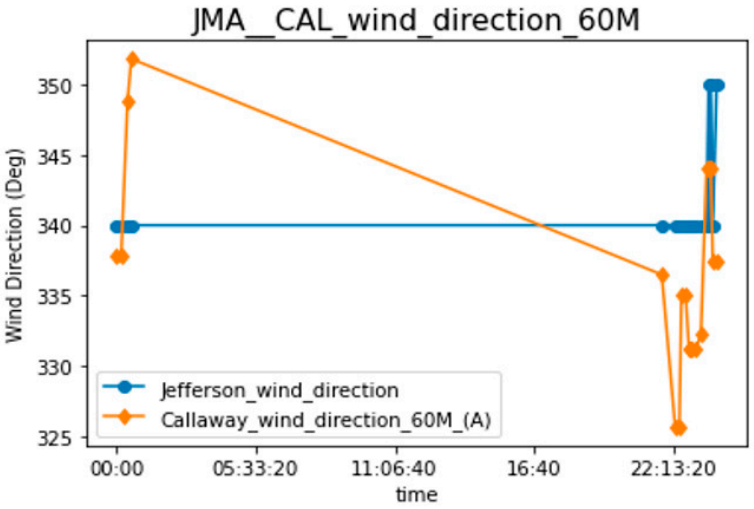

Figure 14. Wind Direction Graph for wind travelling from Jefferson City Memorial Airport to Callaway at 60 m (19 January 2020, data).

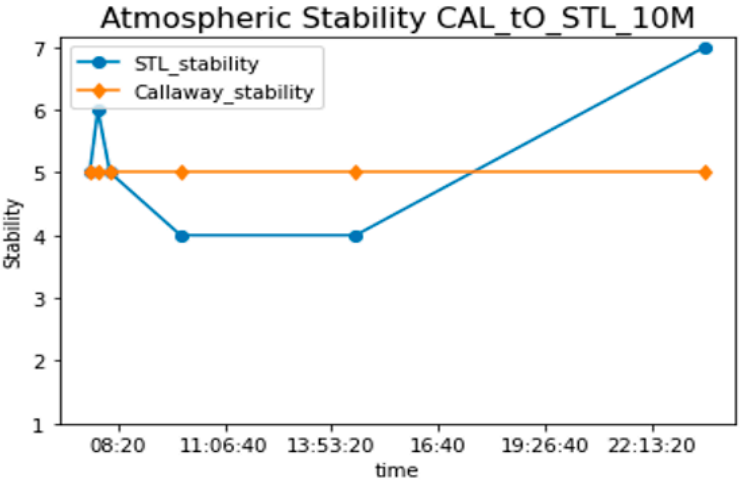

Figure 15. Atmospheric Stability Graph for wind travelling from Callaway to St. Louis Lambert International Airport at 10 m (2 January 2020, data).

Table 14. Atmospheric Data for Callaway Nuclear Power Plant to St. Louis Lambert International Airport for January 2 with Adjustments for Travel Time and Wind Direction at 10 m at Met. T Alpha.

Callaway Time	Callaway Wind Direction in Number 10 m (A)	Callaway Hourly Wind Speed (m/s) at 10 m (A)	Callaway Stability (ΔT) [a] 60 m and 10 m	Travel Time	Arrival Time	St. Louis Lambert International Airport Time	STL Solar Elevation Corrected for Atm Refraction (deg)	STL Hourly Wind Direction (deg)	STL Wind Speed (m/s)	STL Stability Letters
2 January 2020 21:30:00	60.0 (NE [b])	1.3	E (5)	1 days 12:27:50	4 January 2020 09:57:51	4 January 2020 09:55:31	14.1	300 (NW [b])	4.9	D (4)
2 January 2020 21:45:00	36.8 (NE [b])	1.2	E (5)	1 days 16:46:21	4 January 2020 14:31:21	4 January 2020 14:30:31	25.5	280 (W [b])	6.7	D (4)
2 January 2020 20:15:00	39.4 (NE [b])	0.9	E (5)	2 days 03:21:29	4 January 2020 23:36:30	4 January 2020 23:35:31	−64.8	0 (N [b])	0	G (7)
2 January 2020 19:45:00	112.2 (E [b])	0.6	E (5)	2 days 11:51:10	5 January 2020 07:36:10	5 January 2020 07:35:31	−8.6	190 (S [b])	3.6	E (5)
2 January 2020 22:00:00	70.5 (E [b])	0.6	E (5)	2 days 09:48:50	5 January 2020 07:48:50	5 January 2020 07:45:31	−6.8	180 (S [b])	2.7	F (6)
2 January 2020 19:15:00	33.4 (NE [b])	0.4	E (5)	4 days 12:52:39	7 January 2020 08:07:39	7 January 2020 08:05:31	−3.2	280 (W [b])	6.3	E (5)

[a] Temperature variation with height (same footnote for Tables 10–15). [b] Best estimate for the wind direction (same footnote for Tables 10–15).

Figure 15 shows a reasonable correlation between the stability classes for wind traveling from Callaway to St. Lambert International Airport. In most instances, the stability classes match between the two locations. However, there are some discrepancies where the stability classes differ (D (4) at St. Lambert, E (5) at Callaway for two instances, G (7) at STL, and E (5) at Callaway for one instance). Overall, there seems to be a moderate correlation between the stability classes at these two locations, with most instances matching.

Table 15 and Figure 16 shows disparity in the stability classes between the wind travelling from St. Louis Lambert International Airport (STL) to Callaway. The distance between STL and Callaway introduces the possibility of significant variations in local meteorological conditions. Atmospheric stability is influenced by factors such as terrain, topography, and local weather phenomena. Therefore, the distinct stability classes calculated at STL and Callaway are a result of their unique microclimates and geographical features. Additionally, the substantial travel times in stability class observations introduce the potential for changing weather patterns during the travel time. Figures 17–19 show stability, wind speed, and direction comparison for 2 January 2020 between STL and Callaway without any correction for travel time or direction.

Table 15. Atmospheric Data for St. Louis Lambert International Airport to Callaway Nuclear Power Plant for 2 January with Adjustments for Travel Time and Wind Direction at 10 m at Met. T Alpha.

St. Louis Lambert International Airport Time	STL Solar Elevation Corrected for Atm Refraction (deg)	STL Hourly Wind Direction (deg)	STL Wind Speed (m/s)	STL Stability	Travel Time	Arriva Time	Callaway's Time	Callaway Wind Direction in Number 10 m (A)	Callaway Hourly Wind Speed (m/s) at 10 m (A)	Callaway Stability (ΔT) [a] 60 m and 10 m
2 January 2020 01:20:31	−73.9	210 (SW [b])	5.8	E (5)	0 days 08:18:29	2 January 2020 09:39:00	2 January 2020 09:30:00	177.3 (S [b])	3.66	E (5)
2 January 2020 12:20:31	27.5	210 (SW [b])	4.5	C (3)	0 days 10:48:02	2 January 2020 23:08:33	2 January 2020 23:00:00	278.2 (W [b])	0.91	E (5)

Table 15. *Cont.*

St. Louis Lambert International Airport Time	STL Solar Elevation Corrected for Atm Refraction (deg)	STL Hourly Wind Direction (deg)	STL Wind Speed (m/s)	STL Stability	Travel Time	Arriva Time	Callaway's Time	Callaway Wind Direction in Number 10 m (A)	Callaway Hourly Wind Speed (m/s) at 10 m (A)	Callaway Stability (ΔT) [a] 60 m and 10 m
2 January 2020 11:10:31	22.8	210 (SW [b])	3.6	C (3)	0 days 13:30:02	3 January 2020 00:40:34	3 January 2020 00:30:00	346.2 (N [b])	1.09	E (5)
2 January 2020 12:15:31	27.3	210 (SW [b])	3.1	C (3)	0 days 15:25:46	3 January 2020 03:41:17	3 January 2020 03:30:00	12.28 (N [b])	3.48	E (5)
2 January 2020 13:40:31	27.8	210 (SW [b])	3.1	C (3)	0 days 15:25:46	3 January 2020 05:06:17	3 January 2020 05:00:00	357.2 (N [b])	5.27	E (5)
2 January 2020 22:50:31	−57.2	210 (SW [b])	1.8	D+ (4)	1 days 03:00:05	4 January 2020 01:50:37	4 January 2020 01:45:00	274.4 (W [b])	4.11	E (5)
2 January 2020 22:15:31	−50.6	210 (SW [b])	1.3	G (7)	1 days 12:00:07	4 January 2020 10:15:38	4 January 2020 10:15:00	295.5 (NW [b])	3.85	D (4)

[a] Temperature variation with height (same footnote for Tables 10–15). [b] Best estimate for the wind direction (same footnote for Tables 10–15).

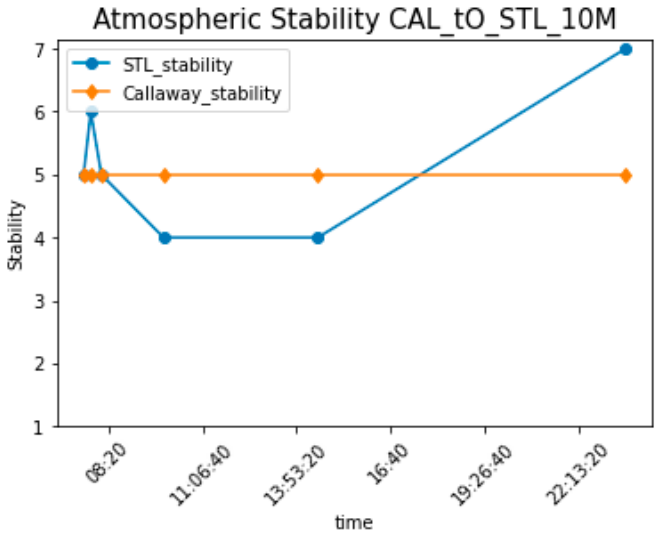

Figure 16. Atmospheric Stability Graph for wind travelling from St. Louis Lambert International Airport to Callaway at 10 m (2 January 2020, data).

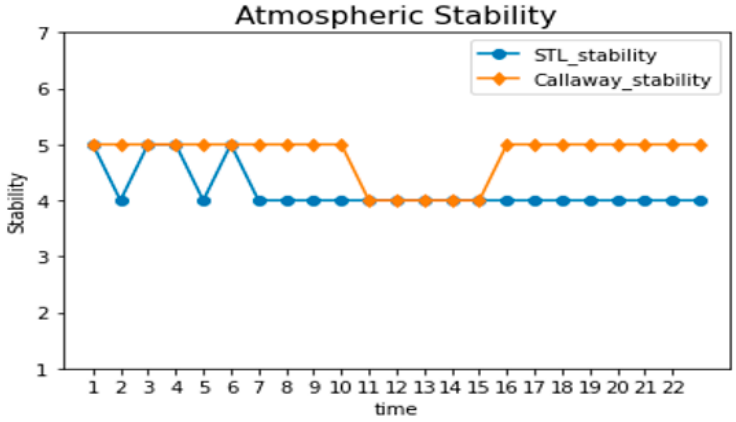

Figure 17. Atmospheric Stability Graph for Callaway and St. Louis Lambert International Airport at 10 and 60 m without Adjustments for Travel Time and Wind Direction (2 January 2020, data).

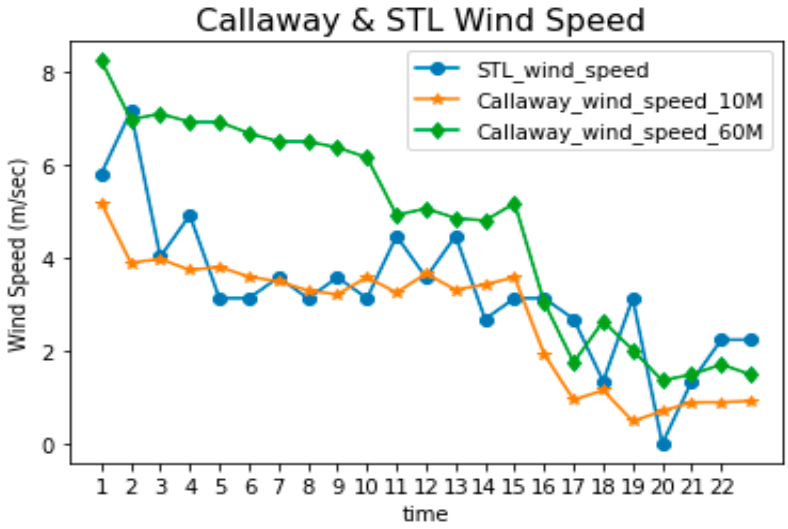

Figure 18. Wind Speed Graph for Callaway and St. Louis Lambert International Airport at 10 and 60 m without Adjustments for Travel Time and Wind Direction.

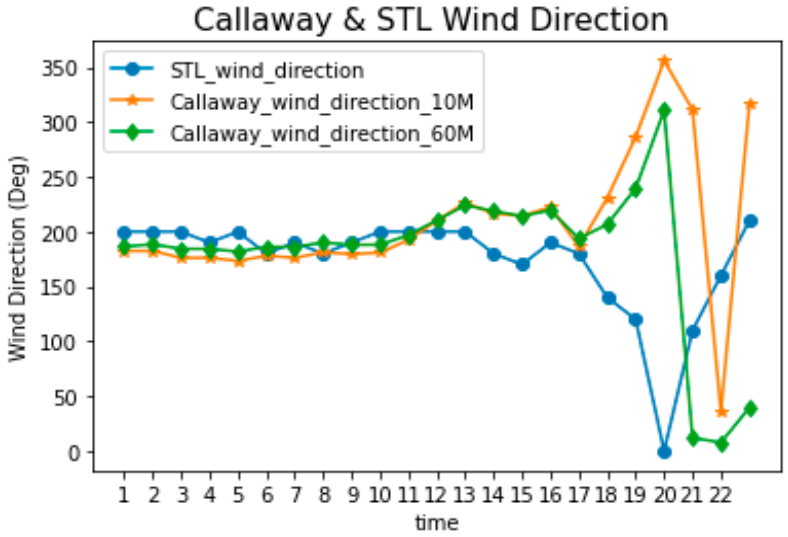

Figure 19. Wind Direction Graph for Callaway and St. Louis Lambert International Airport at 10 and 60 m without Adjustments for Travel Time and Wind Direction.

4. Conclusions

This paper demonstrates the feasibility of automatic procedures for extracting and synthesizing meteorological data from multiple sources, enhancing the availability and reliability of data for regulatory compliance purposes. Reliable off-site data sources can be critical in Emergency Management for existing nuclear power plant when on-site data may become unavailable during a postulated accident condition. This can provide significant guidance to the licensee in managing potential atmospheric release. Similarly, atmospheric data supplementation can significantly accelerate the site licensing process for new licenses as well as for the regulator to effectively evaluate new license applications. By the very nature of atmospheric data, large variabilities and uncertainties are associated with meteorological data collected from any source. Furthermore, there are challenges in integrating data from diverse sources with disparities in formats and collection frequencies.

Our exercise of inferring data from nearby airport was very successful within these bonds of uncertainties. The following conclusions can be drawn from our results.

- Most licensees rely on a vertical temperature gradient $\left(\frac{\Delta T}{\Delta z}\right)$ approach to infer stability class. The use of alternative methods such as proposed by researchers like McElroy and Vogt is equally effective.
- It is quite feasible to utilize already available data in the public domain to obtain useful information for radiological assessment. It was possible for us to infer stability class from the available data of the cloud cover, the date of the year, and the time of the day (the Vogt method) for airports surrounding our reference nuclear site. These predicted stability classes were mostly within one stability class difference from on-site observation at the reference nuclear power plant.
- There is a need for developing carefully designed protocols and methodologies for data integration from various sources. With such tools, reliability and consistency data synthesis is possible. However, for each new site, careful examination of data before integration is necessary.
- Correlation coefficients for velocity and wind directions were also in reasonable agreement for the reference site and the airport locations in the proximity of the reference site.
- Because of the chaotic nature atmospheric flow, there was no significant improvement when applying travel time correction and/or wind direction correction on the net value of correlation coefficients.
- Historical data from reference plant and the off-site locations can be used to develop and validate reliable correlation models. The models need to be continuously evaluated and updated using new available data.
- For a new site, the implementation of this technique includes (1) identification of suitable offsite weather stations and airports with reliable meteorological data, (2) collecting limited onsite data and testing the hypothesis that a temporal–spatial correlation exists between offsite and onsite data, and (3) determining the correlation coefficient and uncertainty of said correlation.
- While NRC does allow for offsite data utilization to demonstrate regulatory compliance, nuclear industry only relies on their onsite meteorological data. There are no examples in the literature of using offsite data for either new COL application or operational compliance. Our work has demonstrated feasibility of utilizing offsite data. This approach can significantly help the nuclear industry.

Author Contributions: Conceptualization, S.U.; methodology, S.U., J.S.; software, B.S.; validation, S.U., S.K., and J.W.; formal analysis, B.S., and S.U.; investigation, B.S, S.K., J.W. and S.U.; resources, S.K., and J.W.; data curation, B.S.; writing—original draft preparation, B.S.; writing—review and editing, S.U.; visualization, B.S.; supervision, S.U and J.S.; project administration, S.U.; funding acquisition, S.U., J.W. and J.S. All authors have read and agreed to the published version of the manuscript.

Funding: Funding for initiating this project was provided as a seed grant by Taylor Geospatial Institute (TGI) based in Saint Louis, Missouri and Ameren Callaway Energy Center. This work was also supported by the Nuclear Regulatory Commission (NRC) at Missouri University of Science and Technology through the NRC fellowship awarded to the first author.

Data Availability Statement: Most of the meteorological data used in this study is public available at request from the weather stations. Raw data from Callaway Nuclear Plant used for this study will be available upon request while the summary of the meteorological data from all nuclear power plants including Callaway can be obtained from NRC open access web page.

Acknowledgments: We acknowledge from Callaway Nuclear Power Plant for providing the required data and explanation of the data acquisition system.

Conflicts of Interest: The authors declare no conflict of interest.

Nomenclature

CNPP	Callaway Nuclear Power Plant
CRA	Columbia Regional Airport
JMA	Jefferson City Memorial Airport
STL	St. Louis Lambert International Airport
NRC	Nuclear Regulatory Commission
COL	Combine License
JFD	Joint Frequency Distribution
Met. T	Meteorological Tower
ΔT	Vertical Temperature Gradient (K)
$\frac{\Delta T}{\Delta z}$	Change in temperature with height (K/m)
Ψ	Pollutant Concentration $\left(\frac{g}{m^3}\right)$
Q	Release Rate (g/s)
$\overline{u}$	Mean Wind Speed (m/s)
σ_y	Horizontal Dispersion Coefficient (m)
σ_z	Vertical Dispersion Coefficient (m)
y	Crosswind Distance (m)
z	Vertical Distance (m)
H	Effective Stack Height (m)
L	Monin and Obukhov Length (m)
u_*	Friction Velocity (m/s)
ρ	Air Density $\left(\frac{kg}{m^3}\right)$
C_p	Specific Heat at Constant Pressure $\left(\frac{J}{kg/K}\right)$
k	Von Karman's constant (Dimensionless)
H	Vertical Heat Flux $\left(\frac{W}{m^2}\right)$
$\sigma_{stability}$	dispersion coefficient (a function of atmospheric stability)
Ri_B	Bulk Richardson Number (Dimensionless)
g	Gravitational Acceleration $\left(\frac{m}{s^2}\right)$
T	Absolute Temperature (K)
$\frac{\partial T}{\partial z}$	Temperature Gradient (K/m)
Γ	Lapse Rate (K/m)
Z	Vertical Distance (m)
u_z	Wind Speed at Height Z (m/s)
α	Sun Elevation Angle
β	Wind velocity correction exponent
δ	Declination Angle
d	Number of days
φ	Latitude
LST	Local Solar Time
HRA	Hour Angle
$u(z)$	Wind Speed at Height z (m/s)
$u(z_0)$	Wind Speed at Reference Height z_0 (m/s)
z_0	Reference Height (m)

Appendix A

Below are graphs illustrating the computed atmospheric stability data for Callaway at Met. T Alpha and the different airports over the entire month of January.

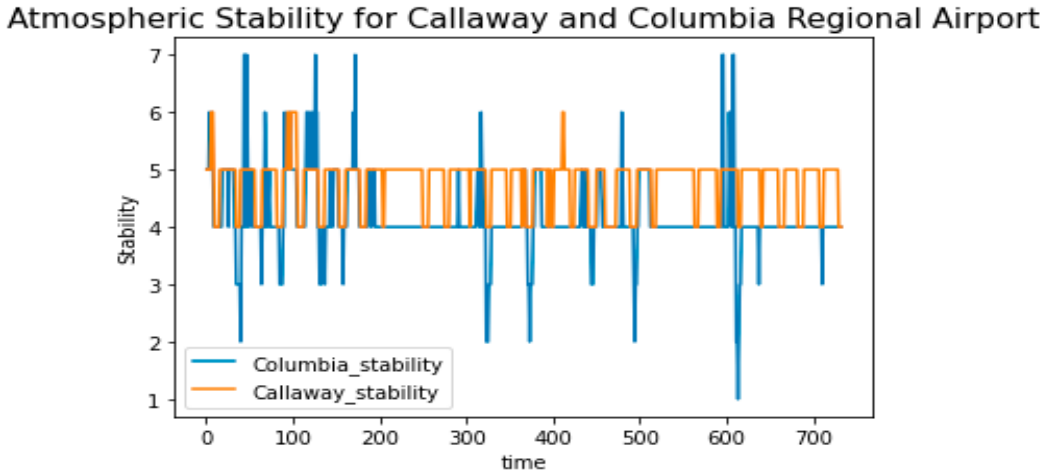
Atmospheric Stability for Callaway and Columbia Regional Airport
Stability
time
Columbia_stability
Callaway_stability

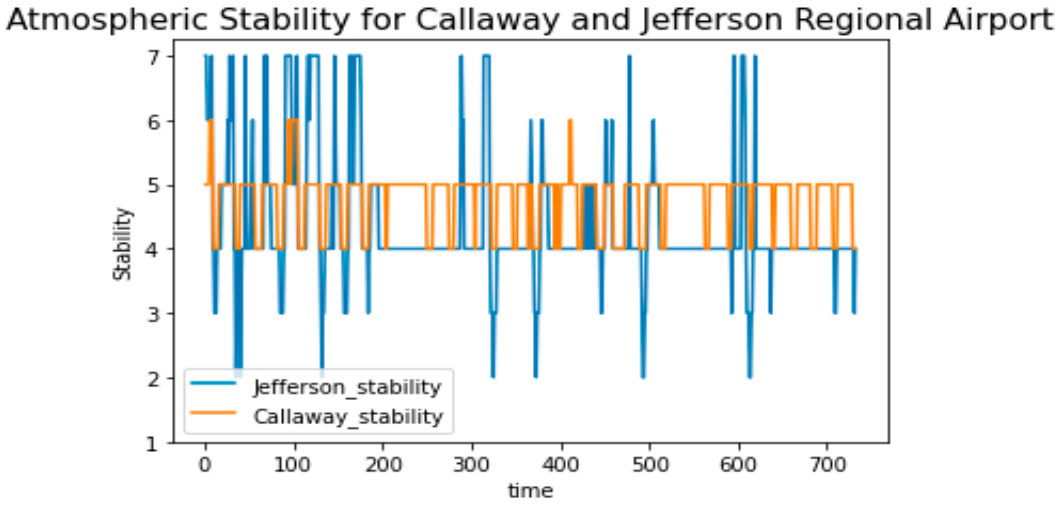
Atmospheric Stability for Callaway and Jefferson Regional Airport
Stability
time
Jefferson_stability
Callaway_stability

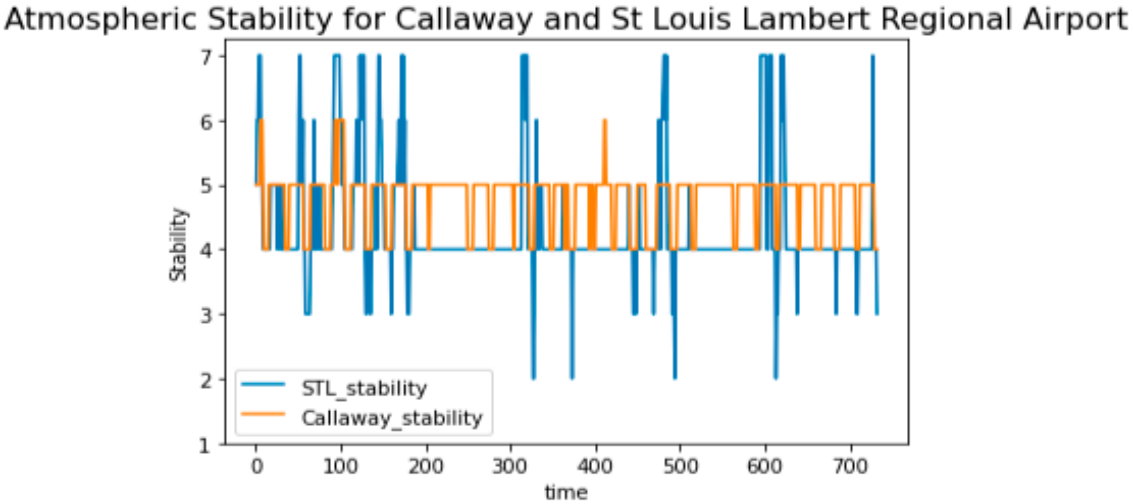
Atmospheric Stability for Callaway and St Louis Lambert Regional Airport
Stability
time
STL_stability
Callaway_stability

Appendix B

Stability Correlation Coefficients between Callaway Nuclear Power Plant and Columbia Regional Airport for January 2020.

Days	CAL and CRA	CAL to CRA at 10 m	CRA to CAL at 10 m	CAL to CRA at 60 m	CRA to CAL at 60 m
1 January	0.69	0	0	0	0
2 January	0.66	0	0	0	0
3 January	0.45	−0.25	0	0.42	0
4 January	0.71	0.34	0	0.39	0
5 January	0.60	0.88	0	0.83	0
6 January	0.58	0	−0.26	0	0.07
7 January	0.66	0.42	0	0.81	0
8 January	0.61	0	0.17	0	0.36
9 January	0.10	0	0	0	0
10 January	0	0	0	0	0
11 January	0	0	0	0	0
12 January	0	0	0	0	0
13 January	0.06	0	0.55	0	0.55
14 January	0.83	0	0	−0.22	0
15 January	0	0	0	0.29	0
16 January	0.79	−0.35	0	−0.26	0
17 January	0.14	0	0.15	0	0.16
18 January	0	0.30	0	0.29	0
19 January	0.67	0.43	0	0.65	0
20 January	0.24	0.08	0	−0.16	0
21 January	0.63	0.61	0	0	0.50
22 January	0.35	−0.10	0	0	0.27
23 January	0	0	0	0	0
24 January	0	0	0	0	0
25 January	0.14	−0.11	0	0.19	0
26 January	0.62	−0.23	0.24	0	0.18
27 January	−0.07	−0.04	0	−0.03	0
28 January	0	0	0	0	0
29 January	0	0	0	0	0
30 January	0.40	0	0	0	−0.14
31 January	0	0	0	0	0

Wind Speed Correlation Coefficients between Callaway Nuclear Power Plant and Columbia Regional Airport for January 2020.

Days	CAL and CRA	CAL to CRA at 10 m	CRA to CAL at 10 m	CAL to CRA at 60 m	CRA to CAL at 60 m
1 January	0.87	0	0	0.41	0
2 January	0.93	0.17	0	−0.05	0
3 January	0.11	0.34	0	0.62	0
4 January	0.72	0.64	0	0.71	0
5 January	0.96	0.74	0	0.69	0
6 January	0.68	−0.55	0.11	−0.72	−0.11
7 January	0.79	−0.10	0	−0.04	0
8 January	0.59	−0.80	−0.06	0.77	0
9 January	0.77	0	−0.51	0	−0.42
10 January	0.45	0.25	−0.06	0.62	−0.35
11 January	0.69	0.67	0	0.60	0
12 January	0.68	−0.65	0.47	−0.63	0.54
13 January	0.05	0	−0.08	0	0.69
14 January	−0.30	−0.73	−0.26	−0.65	0.04
15 January	0.76	0.25	0.48	0.42	0.39
16 January	0.85	0.18	0.27	0.50	0.31
17 January	0.21	0	0.14	0	0.17
18 January	0.66	0.29	0.47	0.14	−0.47
19 January	0.66	0.57	0	0.70	0
20 January	−0.02	0.01	0	0.10	0
21 January	0.91	0	0.13	0	0.52
22 January	0.22	0	0.16	0	0.19
23 January	0.88	0	0.58	0	0.77
24 January	0.82	−0.17	0	−0.11	0
25 January	0.59	0.39	0	0.64	0
26 January	0.52	0.14	0.02	−0.23	0.24
27 January	0.38	−0.21	−0.39	−0.34	−0.49
28 January	−0.08	0	0.10	0	−0.27
29 January	0.68	0	0.27	0	−0.82
30 January	0.42	0	−0.20	0	−0.39
31 January	0.52	0	0.08	0.87	−0.08

Wind Direction Correlation Coefficients between Callaway Nuclear Power Plant and Columbia Regional Airport for January 2020.

Days	CAL and CRA at 10 m	CAL and CRA at 60 m	CAL to CRA at 10 m	CRA to CAL at 10 m	CAL to CRA at 60 m	CRA to CAL at 60 m
1 January	0.57	0.46	0	0	0.30	0
2 January	−0.27	0.16	0.37	0	0.10	0
3 January	0.09	0.30	−0.22	0	0.10	0
4 January	0.90	0.90	0.50	0	0.66	0
5 January	0.90	0.85	−0.04	0	0	0
6 January	0.43	0.71	−0.54	−0.01	0.84	0.13
7 January	0.80	0.71	0.46	0	0.18	0

Days	CAL and CRA at 10 m	CAL and CRA at 60 m	CAL to CRA at 10 m	CRA to CAL at 10 m	CAL to CRA at 60 m	CRA to CAL at 60 m
8 January	0.68	0.69	0.11	0.52	0.15	0.74
9 January	0.64	0.76	0	−0.18	0	−0.12
10 January	0.29	0.23	0.17	−0.27	0.95	−0.07
11 January	0.69	0.40	0.57	0	0.60	0
12 January	0.65	0.68	−0.14	0.17	0.25	0.10
13 January	0.67	0.69	0	−0.02	0	0.34
14 January	0.51	0.74	−0.65	−0.07	−0.26	0.32
15 January	0.86	0.90	0.14	0.05	0.28	−0.08
16 January	0.17	0.15	0.21	0.31	0	0.50
17 January	0.83	0.83	0	0.81	0	0.89
18 January	0.76	0.74	0.59	0	0.55	0
19 January	0.73	0.77	0.07	0	0.41	0
20 January	−0.16	−0.03	−0.33	0	0.16	0
21 January	0.13	0.17	0	0.20	0	0.61
22 January	0.22	0.19	0	0.11	0	0.26
23 January	0.86	0.79	0	0.34	0	0.29
24 January	0.41	0.39	0.16	0	0	0
25 January	0.68	0.46	0.45	0	0.54	0
26 January	0.66	0.64	−0.01	0.32	0.12	0.54
27 January	0.48	0.46	−0.13	−0.05	0.10	−0.33
28 January	0.46	0.41	0	0.28	0	−0.03
29 January	0.10	0.16	0	0	0	0
30 January	0.20	0.66	0	−0.02	0	−0.39
31 January	0.73	0.72	0	0.28	0	0.08

Appendix C

Stability Correlation Coefficients between Callaway Nuclear Power Plant and Jefferson City Memorial Airport for January 2020.

Days	CAL and JMA	CAL to JMA at 10 m	JMA to CAL at 10 m	CAL to JMA at 60 m	JMA to CAL at 60 m
1 January	0.74	−0.25	0.03	−0.19	−0.19
2 January	0.44	0.17	−0.50	0.22	0.05
3 January	0.52	0.81	0.06	−0.86	0.24
4 January	0.73	−0.03	−0.43	−0.16	0.46
5 January	0.60	0.21	−0.25	0.27	−0.17
6 January	0.69	0.24	0	0.16	−0.03
7 January	0.73	0.27	−0.33	0.31	0
8 January	0.70	0	0.01	0	−0.08
9 January	0.12	0.05	0	0.07	0
10 January	0	0	0	0	0
11 January	0	0	0	0	0
12 January	0	0.16	0	0.23	0
13 January	0.08	0	0.11	0	0.07
14 January	0.76	0.42	0	0.42	−0.45
15 January	0	0	0	−0.03	0
16 January	0.76	0	−0.32	0	−0.10

Days	CAL and JMA	CAL to JMA at 10 m	JMA to CAL at 10 m	CAL to JMA at 60 m	JMA to CAL at 60 m
17 January	0.14	0	0.04	0	0.14
18 January	0.09	−0.04	0	−0.01	0
19 January	0.77	0	−0.44	0	0
20 January	0.52	0	0	0	0
21 January	0.69	0.08	0.70	0.14	0.74
22 January	0.35	0.32	−0.71	0.20	−0.71
23 January	0	0	0	0	0
24 January	0	0.13	0	0.08	0
25 January	0.06	0.20	0	0.17	0
26 January	0.64	−0.41	0.33	−0.15	−0.33
27 January	−0.08	0	−0.03	0	−0.04
28 January	0	0	−0.15	0	−0.05
29 January	0	0	−0.10	0	−0.21
30 January	0.59	0	−0.06	0	−0.11
31 January	0.43	0	−0.22	−0.31	−0.22

Wind Speed Correlation Coefficients between Callaway Nuclear Power Plant and Jefferson City Memorial Airport for January 2020.

Days	CAL and JMA	CAL to JMA at 10 m	JMA to CAL at 10 m	CAL to JMA at 60 m	JMA to CAL at 60 m
1 January	0.83	−0.10	−0.43	0.18	−0.34
2 January	0.68	−0.21	−0.12	−0.25	0.15
3 January	0.32	0.13	0.09	0.34	−0.14
4 January	0.75	0.57	−0.62	0.77	−0.54
5 January	0.79	0.64	−0.02	0.53	−0.24
6 January	0.40	−0.41	−0.12	−0.32	0.06
7 January	0.88	−0.14	0.26	−0.05	0.77
8 January	0.76	−0.77	−0.23	0	0.28
9 January	0.69	0.84	0	0.83	0
10 January	0.57	0.08	0.23	0.02	0.13
11 January	0.07	0.24	0.21	0.03	−0.01
12 January	0.52	−0.64	0.10	−0.49	0.08
13 January	0.03	−0.73	−0.20	−0.04	0.10
14 January	0.43	0.80	0.20	0.74	0.23
15 January	0.83	−0.29	−0.44	−0.16	−0.15
16 January	0.55	0	0.30	0	0.35
17 January	0.40	0	0.19	0	0.23
18 January	0.77	0.18	−0.50	0.12	−0.36
19 January	0.62	0	0.52	0	0.14
20 January	0.14	0	−0.84	0	0.66

Days	CAL and JMA	CAL to JMA at 10 m	JMA to CAL at 10 m	CAL to JMA at 60 m	JMA to CAL at 60 m
21 January	0.84	−0.29	0.36	0.16	0.68
22 January	0.28	0.04	0.22	−0.50	0.13
23 January	0.70	0	0.64	0	0.66
24 January	0.88	0.15	0	0.27	0
25 January	0.61	0.48	0	0.57	0.21
26 January	0.50	0.71	−0.26	0.33	0.77
27 January	0.60	−0.57	0.24	−0.60	0.28
28 January	−0.05	0	−0.12	0	−0.10
29 January	0.17	0	0.20	0	0.31
30 January	0.46	0	0.46	0	−0.36
31 January	0.51	0.25	0.04	0.36	−0.07

Wind Direction Correlation Coefficients between Callaway Nuclear Power Plant and Jefferson City Memorial Airport for January 2020.

Days	CAL and JMA at 10 m	CAL and JMA at 60 m	CAL to JMA at 10 m	JMA to CAL at 10 m	CAL to JMA at 60 m	JMA to CAL at 60 m
1 January	0.13	−0.13	−0.37	−0.04	0.10	−0.13
2 January	−0.14	−0.16	0.39	−0.29	0.27	−0.01
3 January	0.30	0.20	−0.11	0.10	−0.05	0.22
4 January	0.77	0.76	0.33	0.45	0.31	−0.13
5 January	0.45	0.48	0.12	−0.01	0.46	−0.02
6 January	−0.34	−0.16	−0.07	0.30	0	0.66
7 January	0.57	0.40	0.34	0	0.38	0
8 January	0.60	0.62	0.26	0.01	0	0.28
9 January	0.21	0.20	0.21	0	0.03	0
10 January	0.10	0.02	−0.50	0.16	−0.34	0.17
11 January	0.60	0.38	−0.45	−0.06	−0.65	−0.18
12 January	0.30	0.32	−0.20	−0.17	−0.29	−0.09
13 January	0.19	0	0.18	0.03	−0.18	−0.06
14 January	−0.56	−0.36	0	0.02	−0.17	0.46
15 January	0.85	0.81	0.41	−0.23	0.75	−0.08
16 January	0.60	0.61	0	−0.09	0	−0.05
17 January	0.62	0.64	0	0.59	0	0.65
18 January	0.59	0.58	0.20	−0.10	0.26	−0.08
19 January	0.75	0.78	0	−0.26	0	0.32
20 January	0.13	−0.11	0	0	0	0
21 January	0.49	0.53	−0.48	0.03	−0.51	0.23
22 January	0.31	0.39	0.25	0	−0.22	0
23 January	0.26	0.22	0	−0.18	0	−0.11
24 January	0.52	0.55	0.44	0	0.42	0

Days	CAL and JMA at 10 m	CAL and JMA at 60 m	CAL to JMA at 10 m	JMA to CAL at 10 m	CAL to JMA at 60 m	JMA to CAL at 60 m
25 January	0.24	0.05	0.33	−0.94	0.29	−0.19
26 January	0.76	0.76	−0.08	−0.77	−0.01	−0.77
27 January	0.06	0.05	−0.12	0.01	−0.30	0.08
28 January	0.50	0.47	0	0.14	0	−0.02
29 January	0.12	0.17	0	0.06	0	−0.08
30 January	0.11	0.50	0.78	0.07	−0.22	0.05
31 January	0.31	0.56	0.32	−0.19	0.48	0.02

Appendix D

Stability Correlation Coefficients between Callaway Nuclear Power Plant and St. Louis Lambert International Airport for January 2020.

Days	CAL and STL	CAL to STL at 10 m	STL to CAL at 10 m	CAL to STL at 60 m	STL to CAL at 60 m
1 January	0.65	0.67	−0.35	0	0
2 January	0.24	0	−0.68	0	−0.25
3 January	0.77	−1	−0.08	−0.58	−0.05
4 January	0.61	0	−0.27	0	0.19
5 January	0.76	0	−0.40	0	0.45
6 January	0.68	−0.06	0.73	−0.22	0.24
7 January	0.67	0	−0.09	0	−0.12
8 January	0.64	−0.22	0.57	−0.25	−0.02
9 January	0	0	0	0	0
10 January	0	0	0	0	0
11 January	0	0	0	0	0
12 January	0	0.11	0	0	0
13 January	0	0.18	0.03	0.19	0.01
14 January	0.57	0.03	−0.21	0.10	0
15 January	0.11	0	−0.09	0	−0.06
16 January	0.22	−0.48	−0.37	−0.48	−0.51
17 January	0	0.12	0	0.12	0
18 January	0	0.26	0.28	0	0.33
19 January	0.50	0	−0.40	0	−0.16
20 January	0.53	0.77	0	0.38	−0.38
21 January	0.55	−0.55	0.37	−0.47	−0.43
22 January	0.11	−0.14	0	0	0
23 January	0	0	0	0	0
24 January	0	0	0	0	0
25 January	0.24	0	−0.05	0	0.14
26 January	0.62	0	0.14	0.04	−0.12
27 January	−0.08	0	0.14	0	0.10

Days	CAL and STL	CAL to STL at 10 m	STL to CAL at 10 m	CAL to STL at 60 m	STL to CAL at 60 m
28 January	0	0	−0.21	0	0.49
29 January	0.32	0.23	0	0.20	0
30 January	0.59	−0.01	0	0.04	0
31 January	0.42	0	0	0	0

Wind Speed Correlation Coefficients between Callaway Nuclear Power Plant and St. Louis Lambert International Airport for January 2020.

Days	CAL and STL	CAL to STL at 10 m	STL to CAL at 10 m	CAL to STL at 60 m	STL to CAL at 60 m
1 January	0.84	0.15	0.29	0	0.45
2 January	0.72	0.09	−0.58	0.61	0.09
3 January	−0.03	0	0.23	0.40	0.30
4 January	0.53	0	−0.24	0	−0.41
5 January	0.73	0.47	0.25	0	0.65
6 January	0.24	−0.38	−0.34	−0.12	0.31
7 January	0.73	0	0.12	0	−0.02
8 January	0.57	0.29	−0.31	0.23	−0.59
9 January	0.49	0.85	0	0.87	0
10 January	0.05	0.18	0.72	0.41	0.57
11 January	0.06	0	0.49	0	0.42
12 January	0.67	−0.28	−0.09	−0.18	−0.70
13 January	0.16	−0.75	0.72	−0.35	−0.89
14 January	0.14	0.28	0	0.10	−0.28
15 January	0.77	0	−0.04	0.04	−0.01
16 January	0.84	−0.24	−0.28	−0.04	−0.07
17 January	−0.05	−0.42	0	−0.39	0
18 January	0.64	−0.27	0.45	−0.56	0.18
19 January	0.78	0	0.69	0	0.64
20 January	0.26	−1	−0.39	−0.13	−0.03
21 January	0.60	0.23	−0.03	0.18	−0.41
22 January	0.05	0.42	0	0.12	0
23 January	0.74	−0.14	0	−0.29	0
24 January	0.87	0	−0.11	0.51	0.02
25 January	0.71	0.12	0.54	0	0.72
26 January	0.35	0.18	−0.08	0.22	−0.24
27 January	−0.04	−0.12	−0.09	−0.18	−0.28
28 January	−0.29	−0.07	0.44	0.02	0.25
29 January	0.48	0.46	−0.50	0.48	−0.57
30 January	0.34	−0.23	0.02	−0.16	−0.49
31 January	0.59	0	0	0	0

Wind Direction Correlation Coefficients between Callaway Nuclear Power Plant and St. Louis Lambert International Airport for January 2020.

Days	CAL and STL at 10 m	CAL and STL at 60 m	CAL to STL at 10 m	STL to CAL at 10 m	CAL to STL at 60 m	STL to CAL at 60 m
1 January	0.60	0.53	−0.67	0.49	0	0.63
2 January	−0.27	−0.24	0.29	0	0.37	0
3 January	0.02	−0.17	0	0.08	−0.63	−0.37
4 January	0.68	0.66	0	−0.38	0	−0.37
5 January	0.89	0.83	0.39	−0.11	0	0.61
6 January	0.43	0.48	0.18	−0.49	0.11	−0.12
7 January	0.57	0.43	0	0.61	0	0.37
8 January	0.49	0.49	0.35	0.49	0.28	0.79
9 January	0.71	0.74	0.91	0	0.71	0
10 January	−0.30	−0.17	−0.04	0.05	−0.05	0.28
11 January	0.53	0.60	0	0.55	−0.01	0.58
12 January	0.85	0.87	−0.14	0.23	−0.05	0.17
13 January	−0.03	0.28	−0.08	0.16	−0.03	0.29
14 January	0.51	0.29	−0.13	−0.42	−0.21	0.14
15 January	0.90	0.95	−0.06	0	0.21	−0.20
16 January	−0.11	−0.07	0.17	−0.16	0.88	−0.03
17 January	0.88	0.89	0.89	0	0.41	0
18 January	0.85	0.85	−0.19	0.65	0	0.74
19 January	0.51	0.49	0	−0.05	0.18	0.16
20 January	0.29	0.36	0.40	−0.04	−0.07	−0.05
21 January	−0.32	−0.36	0.05	−0.09	−0.06	0.03
22 January	0.41	0.39	−0.13	0	−0.55	0
23 January	0.70	0.76	−0.47	0	0.04	0
24 January	−0.02	−0.03	0.31	0.15	0.04	0.13
25 January	0.23	−0.03	−0.58	−0.16	0	−0.16
26 January	0.589	0.52	−0.05	−0.25	−0.07	−0.01
27 January	−0.16	−0.18	−0.23	0.07	−0.33	−0.18
28 January	−0.20	−0.22	0.05	0.27	0.10	−0.01
29 January	−0.23	−0.22	0.34	0.03	0.37	−0.08
30 January	0.29	−0.03	−0.21	−0.31	−0.13	0.48
31 January	0.24	0.48	0	0	0	0

References

1. Nuclear Power in a Clean Energy System. Available online: https://www.iea.org/reports/nuclear-power-in-a-clean-energy-system (accessed on 16 July 2024).
2. Azam, A.; Rafiq, M.; Shafique, M.; Yuan, J. Towards Achieving Environmental Sustainability: The Role of Nuclear Energy, Renewable Energy, and ICT in the Top-Five Carbon Emitting Countries. *Frontiers* **2021**, *9*, 804706. [CrossRef]
3. From Consideration to Construction: The United Arab Emirates' Journey to Nuclear Power. *IAEA*, 3 February 2015. Available online: www.iaea.org/newscenter/news/consideration-construction-united-arab-emirates-journey-nuclear-power (accessed on 16 July 2024).

4. Backgrounder on the Three Mile Island Accident. NRC Web. Available online: www.nrc.gov/reading-rm/doc-collections/fact-sheets/3mile-isle.html (accessed on 16 July 2024).
5. Chernobyl Accident 1986. World Nuclear Association. Available online: https://world-nuclear.org/information-library/safety-and-security/safety-of-plants/chernobyl-accident (accessed on 16 July 2024).
6. The National Environmental Policy Act as Amended through 3 June 2023. Available online: https://www.energy.gov/sites/default/files/2023-08/NEPA%20reg%20amend%2006-2023.pdf (accessed on 16 July 2024).
7. Environmental Protection Regulations for Domestic Licensing and Related Regulatory Functions, (10 CFR 51). Available online: https://www.nrc.gov/reading-rm/doc-collections/cfr/part051/full-text.html (accessed on 16 July 2024).
8. Meteorological and Hydrological Hazards in Site Evaluation for Nuclear Installations. Available online: https://www-pub.iaea.org/mtcd/publications/pdf/pub1506_web.pdf (accessed on 16 July 2024).
9. IAEA Safety Standards Environmental and Source Monitoring for Purposes of Radiation Protection. Available online: https://www-pub.iaea.org/MTCD/publications/PDF/Pub1216_web.pdf (accessed on 16 July 2024).
10. 4 Meteorology and the Nuclear Industry—A Case Study of Industry/Government Cooperation (2010-90annual_3ccm). Available online: https://ams.confex.com/ams/90annual/techprogram/paper_166528.htm (accessed on 16 July 2024).
11. ANSI/ANS-3.11-2015 (R2020). ANSI Webstore. Available online: https://webstore.ansi.org/standards/ansi/ansians112015r2020 (accessed on 16 July 2024).
12. NRC. Regulatory Guide 1.23, Meteorological Monitoring Programs for Nuclear Power Plants. Available online: www.nrc.gov/docs/ML0703/ML070350028.pdf (accessed on 16 July 2024).
13. Economics of Nuclear Power. World Nuclear Association. Available online: https://world-nuclear.org/information-library/economic-aspects/economics-of-nuclear-power (accessed on 3 June 2024).
14. Data Mining with Meteorological Data by A.R. Chaudhari, D.P. Rana, R.G. Mehta, International Journal of Advanced Computer Research (ISSN (print): 2249-7277 ISSN (online): 2277-7970) Volume-3 Number-3 Issue-11 September-2013. Available online: https://nam02.safelinks.protection.outlook.com/?url=https://www.accentsjournals.org/PaperDirectory/Conference/ICETTR-2013/5.pdf&data=05%7C02%7Cbsg4n@mst.edu%7C0503def568904a93e70708dcab4d0704%7Ce3fefdbef7e9401ba51a355e01b05a89%7C0%7C0%7C638573594641549768%7CUnknown%7CTWFpbGZsb3d8eyJWIjoiMC4wLjAwMDAiLCJQIjoiV2luMzIiLCJBTiI6Ik1haWwiLCJXVCI6Mn0=%7C0%7C%7C%7C&sdata=D677uNF0RK6jJwjI/SyPLpue/eMsoxSnZnjikiyJ/ok=&reserved=0 (accessed on 16 July 2024).
15. Chen, L.; Han, B.; Wang, X.; Zhao, J.; Yang, W.; Yang, Z. Machine Learning Methods in Weather and Climate Applications: A Survey. *Appl. Sci.* **2023**, *13*, 12019. [CrossRef]
16. Becker, R.; Thrän, D. Optimal siting of wind farms in wind energy dominated power systems. *Energies* **2018**, *11*, en11040978. [CrossRef]
17. Callaway, Unit 1, 2020 Annual Radioactive Effluent Release Report–NRC. Available online: www.nrc.gov/docs/ML2111/ML21118B043.pdf (accessed on 16 July 2024).
18. Callaway Energy Center 2021 Annual Radioactive Effluent Release Report. Available online: www.nrc.gov/docs/ML2211/ML22110A036.pdf (accessed on 16 July 2024).
19. NRC 10 CFR 100.10 Subpart A–Evaluation Factors for Stationary Power Reactor Site Applications before 10 January 1997, and for Testing Reactors. Available online: https://www.nrc.gov/reading-rm/doc-collections/cfr/part100/part100-0010.html (accessed on 16 July 2024).
20. Callaway Plant Unit 1, Resubmittal of Supplement to 2018 Annual Radioactive Effluent Release Report. NRC. Available online: www.nrc.gov/docs/ML1919/ML19197A319.html (accessed on 16 July 2024).
21. Smriti, S.; Sinha, I.N. Classification of Air Pollution Dispersion Models: A Critical Review. April 2004. Available online: www.researchgate.net/publication/228712544_CLASSIFICATION_OF_AIR_POLLUTION_DISPERSION_MODELS_A_CRITICAL_REVIEW (accessed on 16 July 2024).
22. Giovannini, L.; Ferrero, E.; Karl, T.; Rotach, M.W.; Staquet, C.; Trini Castelli, S.; Zardi, D. Atmospheric Pollutant Dispersion over Complex Terrain: Challenges and Needs for Improving Air Quality Measurements and Modeling. *Atmosphere* **2020**, *11*, 646. [CrossRef]
23. Inversions. Utah Department of Environmental Quality. 5 January 2024. Available online: https://deq.utah.gov/air-quality/inversions#:~:text=Surface%20temperature%20inversions%20play%20a,leading%20to%20poor%20air%20quality (accessed on 16 July 2024).
24. Finardi, S.; Morselli, M.G. Wind Flow Models over Complex Terrain for Dispersion Calculations. Available online: https://www2.dmu.dk/atmosphericenvironment/cost/docs/cost710-4.pdf (accessed on 16 July 2024).
25. Wang, R.; Cui, K.; Sheu, H.L.; Wang, L.C.; Liu, X. Effects of Precipitation on the Air Quality Index, PM2.5 Levels and on the Dry Deposition of PCDD/Fs in the Ambient Air. *Aerosol Air Qual. Res.* **2023**, *23*, 220417. [CrossRef]
26. 18 Atmospheric Boundary Layer. Available online: www.eoas.ubc.ca/books/Practical_Meteorology/prmet102/Ch18-abl-v102.pdf (accessed on 16 July 2024).
27. Hanna, S.R.; Briggs, G.A.; Hosker, R.P., Jr. Handbook on Atmospheric Diffusion (Technical Report) | OSTI.GOV. 1 January 1982. Available online: www.osti.gov/biblio/5591108/ (accessed on 16 July 2024).
28. Radiological Assessment: A Textbook on Environmental Dose Analyses (NUREG/CR-3332, ORNL-5968). NRC Web. Available online: www.nrc.gov/reading-rm/doc-collections/nuregs/contract/cr3332/index.html (accessed on 16 July 2024).

29. O.G.S. Atmospheric Diffusion. by F. Pasquill. London (Van Nostrand Co.), 1962. Pp. XII, 297; 60s. *Q. J. R. Meteorol. Soc.* **1962**, *88*, 202–203. [CrossRef]
30. McElroy, J.L.; Pooler, F., Jr. *St. Louis Dispersion Study Volume I–Instrumentation, Procedures and Data Tabulations*; U.S. Department of Health Education and Welfare, Consumer Protection and Environmental Health Service National Air Pollution Control Administration: Durham, NC, USA, 1968.
31. Gifford, F.A., Jr. Turbulent Diffusion Typing Schemes—A Review. *Nucl. Saf.* **1976**, *17*, 68–86.
32. Vogt, K.J. Umweltkontamination und Strahlenbelastung durch Radioaktive Abluft aus Kerntechnischen Anlagen. *JUl-Rep.* **1970**, 637-ST.
33. PVEducation. Available online: https://www.pveducation.org/pvcdrom/properties-of-sunlight/elevation-angle (accessed on 16 July 2024).
34. Local Climatological Data (LCD) Dataset Documentation. Available online: www.ncei.noaa.gov/pub/data/cdo/documentation/LCD_documentation.pdf (accessed on 16 July 2024).
35. EPA Regulatory Modeling Applications. Available online: www.epa.gov/sites/default/files/2020-10/documents/mmgrma_0.pdf (accessed on 6 February 2024).